Role of the ubiquitin-proteasome pathway in the inner ear: identification of an E3 ubiquitin ligase for Atoh1

by

Yen-Fu Cheng

Doctor of Medicine
Taipei Medical University, 2000

SUBMITTED TO THE HARVARD-MIT PROGRAM OF HEALTH SCIENCES AND TECHNOLOGY IN PARTIAL FULFILLMENT OF THE REQUIREMENTS FOR THE DEGREE OF

DOCTOR OF PHILOSOPHY IN HEALTH SCIENCES AND TECHNOLOGY AT THE MASSACHUSETTS INSTITUTE OF TECHNOLOGY

SEPTEMBER 2014

Signature redacted

Signature of the Author: _____

Yen-Fu Cheng
Harvard-MIT Program of Health Sciences and Technology
August 29, 2014

Signature redacted

Certified by: _____

Albert Edge, PhD
Associate Professor of Otolaryngology, Harvard Medical School
Thesis Supervisor

Signature redacted

Certified by: _____

Emery Brown, MD, PhD/Director, Harvard-MIT Program of Health Sciences and Technology
Professor of Computational Neuroscience and Health Sciences and Technology
Chairman, Committee for Graduate Students

Role of the ubiquitin-proteasome pathway in the inner ear: identification of an E3 ubiquitin ligase for Atoh1

By

Yen-Fu Cheng

Submitted to Harvard-MIT Program of Health Sciences and Technology
On August 29, 2014, in Partial Fulfillment of the Requirements for the Degree of
Doctor of Philosophy in Health Sciences and Technology

Abstract

Atoh1, the proneural basic-helix-loop-helix transcription factor, is critical for the differentiation of inner ear hair cells. Hair cells do not develop in mice that lack *Atoh1*, and overexpression of the transcription factor in embryonic ears induces differentiation of extra hair cells. The level of *Atoh1* expression is under the control of a Wnt and Notch transcriptional regulatory network to keep the level of mRNA within a narrow range. Once the protein is made, it activates its own expression through an interaction with the *Atoh1* enhancer, such that *Atoh1* transcription is self-perpetuating. Because of this autoregulatory loop, halting transcription of the gene to maintain *Atoh1* at an appropriate level would require that the amount of protein be decreased. Since the ubiquitin-proteasome pathway regulates catabolism of key regulatory proteins, we assessed its role in the degradation of Atoh1.

E3 ubiquitin ligases confer substrate specificity to degradation of proteins by transferring a ubiquitin tag to a specific protein substrate. Using an immunoprecipitation/mass spectrometry screening approach, we identified Huwe1, a HECT domain E3 ubiquitin ligase, as an Atoh1 binding partner. We validated the binding between Atoh1 and Huwe1 through reciprocal co-immunoprecipitation and mass spectrometry. We found that Huwe1 promoted polyubiquitylation of Atoh1 through a lysine 48-linked polyubiquitin chain. Mutation at a catalytic cysteine within the HECT domain of Huwe1 reduced the polyubiquitylation. We also defined a motif in the C-terminus of Atoh1 responsible for interaction with Huwe1. Inhibition of proteasomal activity, as well as Huwe1 depletion, stabilized Atoh1 in the cochlea and resulted in generation of new hair cells in the newborn cochlea.

Thesis Supervisor: Albert Edge, PhD
Title: Associate Professor of Otolaryngology, Harvard Medical School

Acknowledgement

There are several people I wish to thank who have helped me over the years of developing this thesis. Each of the following people has provided me with countless support, encouragement and suggestions through the process.

Thanks to my thesis advisor, Albert Edge, for his persistent effort in working with me and transforming me from a clinician into a physician scientist. I appreciate the challenge and insight he provided, which polish this thesis I can now be proud of. I would like to thank fellow committee members Charles Liberman and William Sewell. Both have taken the time to give me valuable suggestions and help me navigate through my thesis. I also want to thank another committee member, Daniel Finley, for giving me one-on-one class which introduced me into the world of ubiquitin-proteasome pathway. I am also thankful for him serving as a member of the oral qualification committee and thesis committee while giving constant input to my thesis. I also want to thank Wade Harper and John Lydeard for the research support from the mass-spectrometry side.

I am grateful for the financial support I received from the Yen Tjing Ling Medical Foundation (Taiwan), the Foundation for Poison Control (Taiwan), the Ministry of Education (Taiwan), Amelia-Peabody Foundation (Wellesley, MA), the Helen Carr Peake Research Assistantship (MIT), the American Academy of Otolaryngology-Head and Neck Surgery Foundation Percy Memorial Research Award and the American Hearing Research Foundation Wiley H. Harrison Memorial Research Award.

Additionally would like to give my thanks to the members of the Edge Lab for helping me through the whole journey. Specifically, I would like to thank Fuxin Shi, for her teaching me every molecular biological procedure from my first day in the lab and also Judith Kempfle, Marco Petrillo, Danielle Lenz and Vasiliki Zoto for great coffee and lunch meetings. Also thank you to Vasiliki Zoto for helping me with many experiments, to Mark Parker, Marco Petrillo, Danielle Lenz, Will Mclean, Mingjie Tong, Xiankai Meng, and Jingrong Lu for research collaborations. I want to also thank other important members of Edge Lab and Eaton Peabody Lab such as Diana Sands, Shyan-Yuan Kao, Chii-Yuan Huang, Chen-Chi Wu, Masato Fujioka, Kunio Mizutari, Kevin Jiang, Yilai Shu, Yong Tao, Na Lu, Wenyan Li, Jingfang Wu, Mingqian Huang and Kris Kristiansen for their help and friendship.

I want to express my gratitude for my SHBT classmates, Maria Berezina, Gus Halwani, Andrew Lysaght, Sofia Vallila and Bo Zhu, as they shared their best perspectives of knowledge to help me get through the tough first year and made my SHBT life unforgettable. I also want to thank Nelson Kiang for his constructive criticism and comments in regards to my career. Additionally, I would like to thank Ruth Anne Eatock and Konstantina Stankovic for helping me with the oral qualification.

Most importantly I would like to thank my immediate and extended family for their unconditional support. Thanks to my parents, grandparents, and parents-in-law for the love. Yinyin and Elin, for your patience during my long PhD journey, and tolerance of my mood during the writing of my thesis. I could have never done this without your support and love.

This thesis is dedicated to the memory of my beloved father, Mr. Kuang-Ting Cheng (鄭光庭). I would not have the chance to go abroad to study without his encouragement and support. Thank you my dear father for everything.

TABLE OF CONTENTS

List of Figures

Lists of Tables

Introduction

Hearing loss is one of the most prevalent disabilities found in industrialized countries: estimates are that 278 million people have moderate to profound hearing deficiency, worldwide (WHO). More than 80% of all cases of hearing loss can be attributed to the degeneration and death of two specific inner ear cell types: cochlear hair cells, which act as the primary receptors for sound, and their associated spiral ganglion neurons, which transmit electrical signals from the hair cells to the brain (Davis, 1983). Loss of mammalian cochlear hair cells caused by genetic mutations, autoimmune disease, ototoxic medications, exposure to noise, or aging is usually permanent, and there are currently no methods to recover hearing after hair cell damage.

Mammals show limited ability to regenerate hair cells; while vestibular hair cells have a limited regenerative capacity (Forge et al., 1993; Warchol et al., 1993), and no regeneration has been reported in cochlear hair cells. For the deficiency in auditory function due to loss of cochlear hair cells, cochlear implants are surgically implanted in the inner ear to stimulate the spiral ganglion. However, cochlear implants depend on still functioning spiral ganglion neurons, whose loss can severely compromise efficacy (Incesulu and Nadol, 1998). The regeneration or replacement of damaged hair cells in the cochlea is consequently a critical goal for the eventual treatment of hearing loss.

Many approaches have been taken toward hair cell regeneration, such as cell therapy, gene therapy or pharmacological therapy. Although there have been some successful attempts of cell transplantation into the damaged cochlea, most report limited survival of the grafted cells or differentiation into mature hair cells, perhaps due to the complex anatomy and physiology of the cochlea (Hu et al., 2005; Hu and Ulfendahl, 2006). The same anatomical barriers have limited the success of gene therapy of the inner ear, and the lack of ideal vector system as well as appropriate

delivery methods make exogenous gene transfer into the mature inner ear challenging (Husseman and Raphael, 2009). Pharmacotherapy using small molecule compounds, which can manipulate signaling pathways in inner ear stem cell/progenitors with the capacity to differentiate into hair cells for local delivery, seems to be a more physiological approach to regeneration of hair cells (Mizutari et al., 2013). However, this will require a better understanding of the underlying mechanisms controlling hair cell formation.

This thesis presents a new approach to hair cell formation, which is critical to restoring hearing to those with moderate to profound hearing loss. By manipulating signaling pathways regulating Atoh1 protein, and ultimately applying this knowledge to inner ear regeneration, we have demonstrated a new understanding of how cells regulate the level Atoh1 post-translationally to achieve hair cell differentiation. Formation of hair cells is dependent on the protein, Atoh1 (atonal1). Atoh1 is a basic helix-loop-helix (bHLH) transcription factor and is necessary and sufficient for hair cell differentiation both during development and through derivation from stem cells (Bermingham et al., 1999; Jeon et al., 2007). Experiments overexpressing Atoh1 in the inner ear via gene transfer had demonstrated new hair cell formation in the organ of Corti and improved hearing in animals treated with ototoxic aminoglycosides (Izumikawa et al., 2005). Our approach to this problem was to understand how Atoh1 is regulated at the post-translational level, specifically by the ubiquitin-proteasome pathway. We find that by intervening in the post-translational regulatory pathways for the expression of Atoh1 we can direct the differentiation of appropriate stem cells or progenitors into hair cells.

We have recently shown that Wnt and Notch signaling play key roles in inner ear stem cell differentiation. Notch signaling plays a key role in designating the prosensory regions in the otocyst and the differentiation of precursors to hair cells and supporting cells, while Wnt signaling

is important for stem cell maintenance and expansion (Clevers, 2006); it is a key regulator of cell differentiation in the early otocyst (Stevens et al., 2003). We showed previously that β-catenin, the intracellular mediator of Wnt signaling, increases the expression of Atoh1 and that interaction between β-catenin and the Atoh1 enhancer is responsible for increased Atoh1 expression (Shi et al., 2010). We also found that inhibition of Notch signaling by γ-secretase inhibition not only stimulates β-catenin expression in neural progenitor cells (Shi et al., 2010), but also increases hair cell differentiation in inner ear stem cells by its influence on the expression of Atoh1 (Jeon et al., 2011; Mizutari et al., 2013; Bramhall et al., 2014).

To date, some investigations have shown that *Atoh1* expression can be upregulated at the transcriptional level through various signaling pathways (Shi et al., 2010; Jeon et al., 2011; Mizutari et al., 2013; Bramhall et al., 2014), but the cellular post-translational regulatory systems for the Atoh1 protein were, until now, largely unknown, and thus successful regeneration of functional hair cells remained elusive. The ubiquitin-proteasome pathway is the major post-translational regulatory system and has been implicated in the regulation of stem cell differentiation and lineage commitment via proteolytic degradation of key regulatory proteins. Thus we demonstrate here that specific inhibition of the ubiquitin-proteasome pathway stabilizes the level of Atoh1 protein in the inner ear and forces progenitors toward a hair cell fate. This information points to a novel approach to inner ear regeneration. By identifying the effect of the ubiquitin-proteasome pathway on the regulation of Atoh1, this work explains the post-translational regulatory mechanism of Atoh1 and provides biochemical evidence that may ultimately lead to novel clinical interventions for replacement of hair cells in a damaged cochlea and to hearing restoration.

Thesis outline

This thesis is written in five chapters, which include a background chapter, followed by three chapters describing different phases of my research, including two chapters exploring the mechanisms of Atoh1 post-translational regulation, mostly focusing on the ubiquitin-proteasome pathway and the related E3 ubiquitin ligases, and one chapter describing manipulating Atoh1 proteasomal degradation to achieve hair cell generation in the cochlea.

In **Chapter 2,** also the first phase of my research, we investigate the mechanism of Atoh1 degradation. The primary focus of this chapter is to explore biochemical properties of Atoh1 protein stability and mechanisms leading to its degradation. We find that Atoh1 is degraded by the ubiquitin-proteasome pathway through the addition of polyubiquitin chains conjugated at lysine 48 of ubiquitin. We also identify the C-terminus of Atoh1 as the site where signals for proteasomal degradation are found.

In **Chapter 3**, we further dissect the main components of the ubiquitin-proteasome pathway responsible for Atoh1 degradation. We present a proteomic study in collaboration with Dr. Wade Harper's lab to identify the E3 ubiquitin ligase responsible for proteasomal degradation of Atoh1. We find that Huwe1, a HECT domain E3 ubiquitin ligase, interacts with and transfers ubiquitin to Atoh1. We validate the role of Huwe1 in Atoh1 degradation with a series of biochemical studies using mutants of Atoh1 as well as ubiquitin and Huwe1.

In **Chapter 4**, we apply the knowledge gained in the previous two chapters to the manipulation of the proteasomal degradation of Atoh1 toward the aim of hair cell generation in the cochlea. Knocking down Huwe1 expression by RNA interference leads to Atoh1 stabilization and generation of hair cells. These results open up possibilities for a therapy that could be helpful for deaf patients.

Chapter 5 concludes my thesis work and describes future directions.

Chapter 1. Background

I. Inner ear development and regeneration

Cochlear function

Acoustic signals undergo a series of transformations leading to the perception of sound in the auditory cortex. Sound travels through the external ear canal, the tympanic membrane, and the ossicular chain in the middle ear, resulting in movement of the stapes within the oval window and pressure changes within the fluids of the inner ear. This leads to the vibration of the cochlear partition containing the sensory hair cells (Figure 1-1). All hearing sensation is derived from the output of fewer than 15,000 sensory hair cells per inner ear.

These hair cells are the mechanoelectrical transducers of the ear. Displacement of the stereocilia of the hair cells, which occurs due to shearing movements between the tectorial membrane and basilar membrane, is the effective stimulus that initiates the transduction of mechanical vibration to intracellular currents. Receptor potentials of the hair cells initiate chemical changes at the hair cell-neuron synapse and generation of action potentials. Neural impulses propagate through axons of the auditory nerve and to the synapses on cells within the brainstem, beginning a series of neural transformations in the central nervous system.

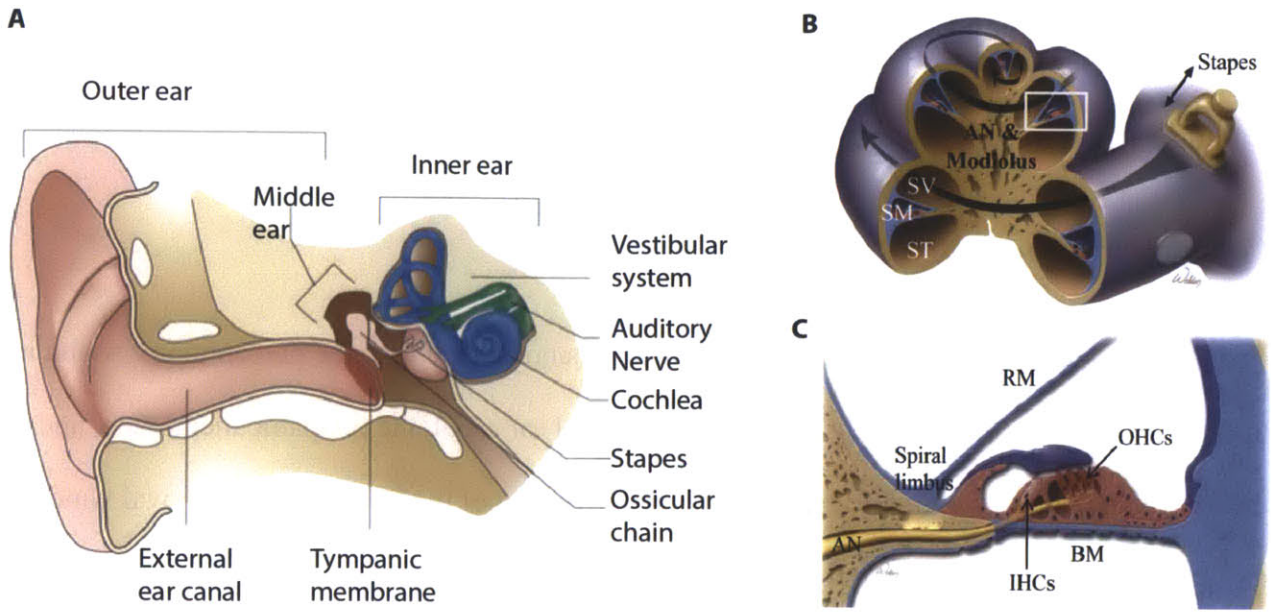

Figure 1-1. The anatomy of the inner ear
A) The outer ear, middle ear and inner ear.
B) The scala vestibuli (SV), scala media (SM) and scala tympani (ST) are fluid-filled chambers of the cochlear partition. The auditory nerve (AN) is located within the modiolus.
C) Cross section of organ of Corti within the cochlear duct. The hair cells and supporting cells in the organ of Corti sit on the basilar membrane (BM). Adapted from Kelley 2006 & Gao et al. 2011)(Kelley, 2006; Gao et al., 2011b).

Anatomy of the inner ear

The cochlea

The mammalian cochlea, which is the hearing organ of the inner ear, is a spiral bony duct embedded in the temporal bone of the skull. Inside the cochlea are three fluid-filled chambers: the scala vestibuli, scala tympani and scala media. The scala vestibuli lies superior to the cochlear duct, the scala tympani inferior, with the organ of Corti containing the hair cell in the scala media between the two. These chambers are separated by Reissner's membrane between the scala vestibuli and scala media, and the basilar membrane between the scala media and the scala tympani (Figure 1-1).

The organ of Corti

The organ of Corti is the sensory epithelium on the basilar membrane of the scala tympani. It transduces amplified sound waves transmitted from the middle ear. The organ of Corti contains both hair cells and supporting cells; the former are apically specialized sensory cells responsible for stimulus transduction, while the latter are specialized for mechanical and metabolic support. The organ of Corti contains three rows of outer hair cells and one row of inner hair cells and the supporting cells surrounding the hair cells (Figure 1-2).

The outer hair cells are supported by Deiters' cells at the base, lying laterally to the outer pillar cells, while the inner hair cells are surrounded by supporting cells, medial to the inner pillar cells. Inner hair cells are the primary receptor cells while outer hair cells serve as amplifiers of sound. Specialized stererocilia at the apex of the cell respond to fluid motion in the scala media via mechanosensing transduction channels responsible for potassium influx from endolymph that causes depolarization to generate neural signals to the brain.

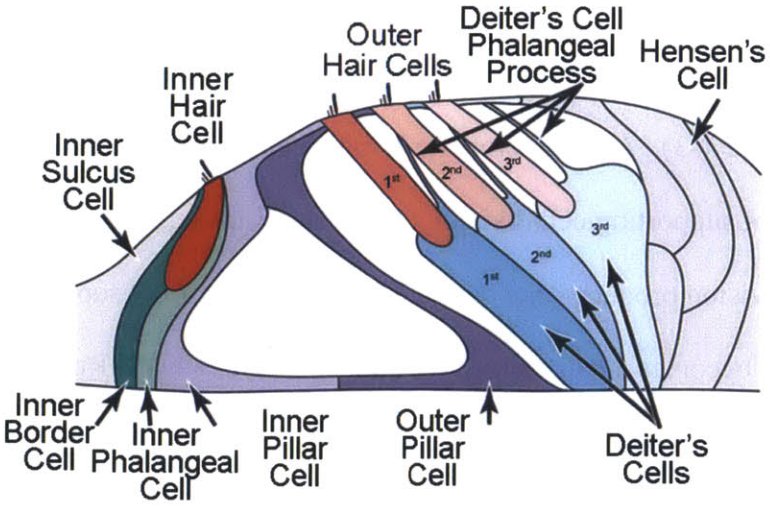

Figure 1-2. Sensory epithelial cells, including supporting cells and hair cells, in the organ of Corti Adapted from Shi (2012).

The vestibular system

The vestibular system is responsible for motion perception. It consists of three semicircular canals to detect angular acceleration of head rotation and two otolith organs to detect linear acceleration and gravity. Vestibular hair cells are surrounded by supporting cells; together they comprise the sensory epithelium of the canal cristae of the semicircular canals and the maculae of the otolith organs. Similar to cochlear hair cells, vestibular hair cells serve as mechanoreceptors to sense fluid motion within the vestibular labyrinth and to convert mechanical stimuli into neural signals directed towards the central nervous system.

Hair cell development and regeneration

Regeneration of hair cells

While mammals display no capacity to regenerate auditory hair cells and limited capacity to regenerate vestibular hairs (Forge et al., 1993; Warchol et al., 1993), birds and fish show continuous turnover of hair cells and regeneration after damage leading to hair cell loss (Corwin and Cotanche, 1988). Two mechanisms in birds have been proposed: direct differentiation and asymmetric cell division (Figure 1-3). After an ototoxic insult, supporting cells are converted into hair cells in the absence of supporting cell division (Adler and Raphael, 1996; Roberson et al., 2004). Supporting cell division produces one daughter cell that becomes a supporting cell, and another daughter cell that becomes a hair cell (Stone and Cotanche, 1994). Regenerated hair cells from transdifferentiation occurs as early as 15 hours after the ototoxic event (Cafaro et al., 2007), followed by mitotic generation of hair cells. Once the cell division mechanism is initiated, direct transdifferentiation is limited, so that most of the new hair cells in the epithelium

occur through the cell division mechanism, and the system can then eventually replenish the supporting cell pool.

Loss of mammalian auditory hair cell is usually permanent. The regeneration or replacement of damaged hair cells in the cochlea is consequently an important goal for the eventual treatment of hearing loss.

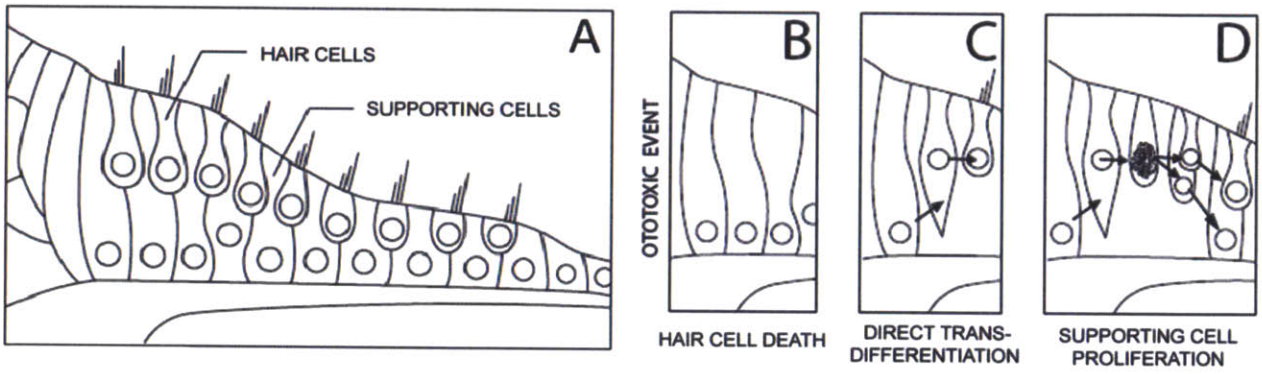

Figure 1-3. Hair cell regeneration in birds
(A&B). After ototoxic damage to the inner ear, hair cells are destroyed and are regenerated from supporting cells.
(C) The first new hair cells are made by direct transdifferentiation of supporting cells.
(D) A second wave of new hair cells, which will dominate the newly generated hair cells in the epithelium, result from cell division to make a new hair cell and a new supporting cell. Adapted from Parker (Parker, 2011).

II. Atoh1, a bHLH transcription factor, is required for hair cell differentiation

Basic helix-loop-helix (bHLH) transcription factors orchestrate cell fate commitment and specification during myogenesis and neurogenesis (Lo et al., 1991; Ross et al., 2003). 39 bHLH transcription factors are encoded in the genome of the worm Caenorhabditis elegans, 58 in the Drosophila melanogaster genome and 125 in the human genome (Ledent et al., 2002). The bHLH transcription factors interact with binding partners and bind to DNA at specific sites known as E-boxes (Murre et al., 1989). A homologous group of "proneural" bHLH transcription factors (Figure 1-4) play a role in neurogenesis. The bHLH domain confers specificity of DNA binding and protein-protein interaction. Several bHLH transcription factors, including Atoh1, Neurog1, NeuroD and Ascl1, contribute to the development of inner ear neurons and hair cells (Bertrand et al., 2002; Fritzsch, 2003; Tiveron et al., 2003).

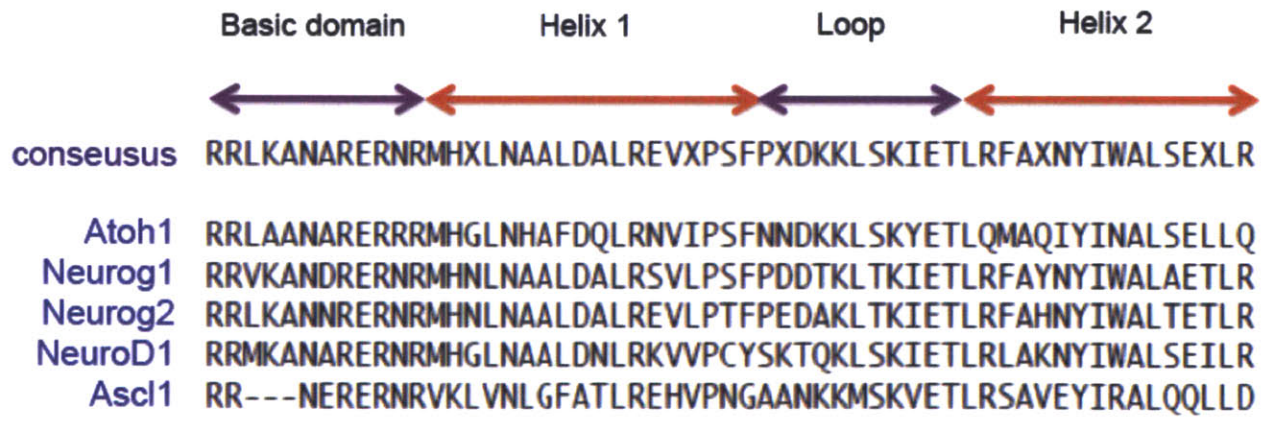

Figure 1-4. Alignment of bHLH domains
bHLH domain sequences of various proneural transcription factors were aligned using Lasergene MegAlign software.

Embryonic *Atoh1*-null mice fail to generate cochlear and vestibular hair cells (Bermingham et al., 1999) as a result of progenitor cell apoptosis in the absence of *Atoh1* (Chen

et al., 2002). In gain-of-function studies, Zheng and Gao overexpressed *Atoh1* and observed extra hair cells in explants of the organ of Corti (Zheng and Gao, 2000). *In vivo* and *in utero* experiments confirmed that forced upregulation of *Atoh1* led to the generation of supernumerary hair cells (Woods et al., 2004; Izumikawa et al., 2005; Staecker et al., 2007; Gubbels et al., 2008), but very little is known about how cells regulate the level of *Atoh1*.

Atoh1 level is important for hair cell development and regeneration

Proper spatiotemporal expression *Atoh1* is critical for the differentiation and viability of hair cells. *Atoh1* is expressed in hair cell progenitors before they commit to the hair cell fate. *Atoh1* is first detected at E13.5 in the basal turn of the developing cochlea. It is strong at the base of the cochlea by E14.5 and appears at the apical turn as late as E17.5. Its expression starts to decline at P0 in hair cells at the basal turn by P4 at the apical turn (Figure 1-5) (Yang et al., 2010a; Pan et al., 2012). *Atoh1* affects hair cell survival, stereocilia maturation and onset of hearing (Pan et al., 2012; Cai et al., 2013). For example, *Atoh1* is critical for the survival of hair cell progenitors at the base of the cochlea for a window of 72 hours, and deletion of *Atoh1* outside this window does not affect survival.

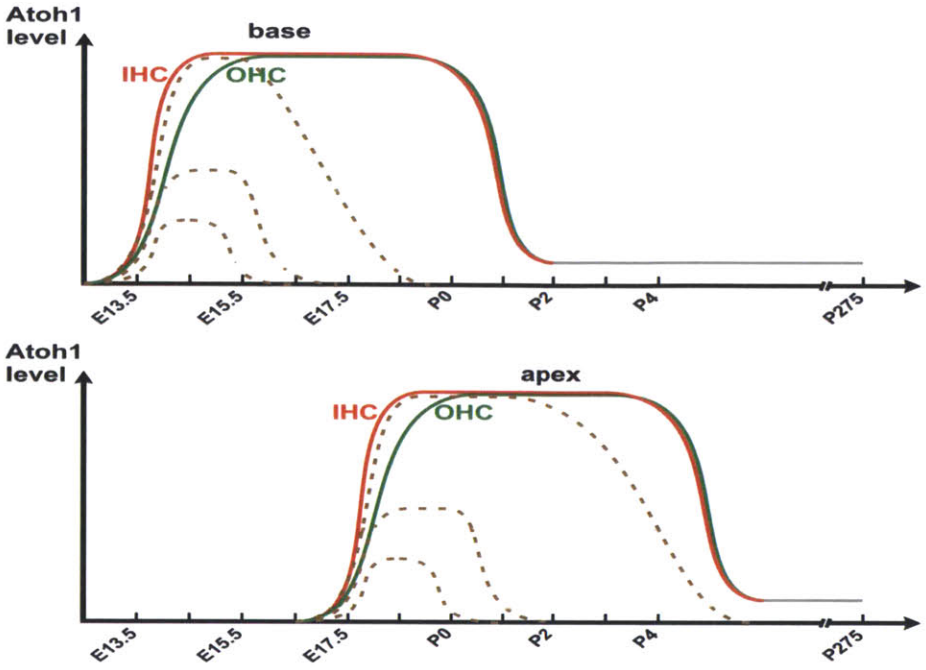

Figure 1-5. Differential expression of Atoh1
Atoh1 is expressed earlier in the base than in the apex, and earlier in IHCs (red line) than in OHCs (green line). Adapted from Pan et al (2012).

Signaling pathways regulating Atoh1

Atoh1 is detectable in the supporting cells of non-mammalian utricles under normal conditions and is rapidly upregulated during regeneration (Cafaro et al., 2007; Ma and Raible, 2009). *Atoh1* transcription has been detected after damage to vestibular supporting cells in mammals *in vitro* (Lin et al., 2011) and *in vivo* (Kawamoto et al., 2009), although very few of the cells that upregulate *Atoh1* go on to express detectable protein or transdifferentiate to hair cells (Lin et al., 2011). *Atoh1* expression after hair cell loss in the mammalian cochlea does not occur spontaneously.

Notch signaling pathway

Notch signaling plays a critical role in inner ear development and *Atoh1* regulation (Jarriault et al., 1995; Lanford et al., 1999; Brooker et al., 2006). The main role of *Notch*

signaling is to mediate interactions between hair cells and supporting cells for cell fate decision during development.

The inner ear is derived from the otic placode, which is recognized initially as a thickening near the hindbrain at embryonic day (E) 8 in mice. The otic placode invaginates by E10.5 forming an otocyst containing prosensory cells and ganglion neuroblasts. Determination of hair cell or supporting cell fate is influenced by Notch signaling. Developing hair cells express *Atoh1* and Notch ligands, Jag2 and Delta1, which bind to Notch1 in adjacent cells and induce the release of Notch intracellular domain (NICD) from the cell membrane. Upregulation of two inhibitory bHLH transcription factors, Hes1 and Hes5, follows, and expression of *Atoh1* is blocked, leading to inhibition of hair cell fate. The inhibited cells develop as supporting cells (Fig. 6) (Kelley, 2006).

Pharmacological inhibition of Notch signaling increases cochlear hair cell number in newborn organ of Corti explants (Yamamoto et al., 2006; Takebayashi et al., 2007) and in inner ear stem cells (Jeon et al., 2011). Treatment of mice with a γ–secretase inhibitor after hair cell loss due to noise damage resulted in hair cell regeneration accompanied by recovery of cochlear function through the upregulation of Atoh1 (Mizutari et al., 2013).

Wnt/beta-catenin signaling pathway

The *Wnt* pathway plays a key role in patterning and cell fate specification in early development of the inner ear (Gregorieff and Clevers, 2005) (Stevens et al., 2003) (Ohyama et al., 2006) (Riccomagno et al., 2005). Wnt binding to a cell increases the level of β-catenin, which translocates to the nucleus, where it mediates canonical Wnt signaling by regulating transcription of target genes.

Stevens et al. found that the Wnt/β-catenin pathway induced patches of vestibular hair cells and supporting cells in the auditory sensory epithelium and was involved in establishing or maintaining distinctions between sensory and non-sensory domains in the inner ear (Stevens et al., 2003). Our lab found that β-catenin increased expression of Atoh1 in neuroblastoma cells and neural progenitor cells (Shi et al., 2010). The upregulation of Atoh1 was caused by an interaction of β-catenin with the Atoh1 3' enhancer. We also found crosstalk between Notch and Wnt/β-catenin signaling pathways: β-catenin expression was increased after inhibition of Notch signaling, and this increase accounted for the effect of Notch inhibition on Atoh1 expression (Shi et al., 2010). β-catenin knockout inhibited hair cell formation from sensory progenitors, while constitutive activation of β-catenin expanded sensory progenitors and resulted in differentiation of extra hair cells (Shi et al., 2012; Shi et al., 2014).

Atoh1 is widely expressed

In addition to hair cell formation, Atoh1 is plays important roles in the differentiation of several other cell types, including goblet cells in the intestinal epithelium (Yang et al., 2001), granule cells in the cerebellum (Ben-Arie et al., 1997; Flora et al., 2007), dorsal commissural interneurons in the spine (Miesegaes et al., 2009) and Merkel cells of the skin (Ben-Arie et al., 2000; Morrison et al., 2009; Maksimovic et al., 2014), all of which are lacking after Atoh1 knockout.

The expression of *Atoh1* has been associated with tumor formation. Atoh1 plays a roles as a tumor suppressor gene in the colon, as Atoh1 antagonizes tumor formation and growth, while colorectal cancer and Merkel cell carcinoma patients show genetic mutations of *Atoh1* (Bossuyt et al., 2009). On the other hand, *Atoh1* acts as an oncogene in medulloblastoma (Flora et al., 2009), indicating its multiple roles in differentiation as well as proliferation in different cell types.

III. Post-translational regulation by the ubiquitin-proteasome pathway

Post-translational modification of proteins can include phosphorylation, acetylation, sumoylation, glycosylation and ubiquitylation. The ubiquitin-proteasome pathway plays an important role in development and physiology of eukaryotic cells (Tai and Schuman, 2008). Specific proteins are labeled by polyubiquitin chains in an energy-consuming process and then targeted to the proteasome where they are degraded to small peptides. The system is highly selective and precisely regulated; it not only degrades misfolded or damaged proteins but is also essential for the regulation of cell-signaling pathways, determining the half-lives of proteins (Naujokat and Šarić, 2007).

The ubiquitin system consists of three critical enzymes: a ubiquitin-activating enzyme (E1), ubiquitin-conjugating enzyme (E2), and ubiquitin ligase (E3). Ubiquitin is covalently conjugated to E1 in an ATP-dependent manner, followed by transfer to E2. E3 catalyzes the formation of polyubiquitin chains (and occasional monoubiquitin chains) by transferring activated by E1 and E2 to internal lysine residues on specific substrates.

Ubiquitin is a 76- amino acid polypeptide containing multiple lysines capable of forming polyubiquitin chain on the substrates. In addition to polyubiquitin chain linked on the lysine at

amino acid 48 (K48), which is a signal for proteasome degradation of ubiquitylated substrate, mono or polyubiquitin chains can be formed through linkages at other positions (K6, K11, K27, K29, K33 or K63)(Peng et al., 2003; Ikeda and Dikic, 2008; Meierhofer et al., 2008). K63 polyubiquitin chains modify substrate activity and activate enzymes of DNA repair (Spence et al., 1995), intracellular signaling(Abbott et al., 2007) and endosomal trafficking (Huang et al., 2013). The functions of some of the linkages have not been well characterized.

E3 ubiquitin ligases are classified by the occurrence of HECT (homologous to the E6-AP C-terminus) or RING (really interesting new gene) domains, based on the identity of the domain involved in E2 ubiquitin conjugation enzyme interaction. The human genome encodes over 600 E3 ligases, most belonging to the RING family (Deshaies and Joazeiro, 2009). HECT domain ligases form a transient and covalent thioester bond with ubiquitin via a conserved cysteine before the substrate ubiquitylation, while RING domain ligases transfer ubiquitin from E2 to the substrate, without a direct ubiquitylation.

HECT E3 ligases are assumed to catalyze the attachment of ubiquitin not only to the substrate but also to ubiquitin (for extension of the ubiquitin chain). The HECT domain is a C-terminal region of 350 amino acids (Huibregtse et al., 1995). The domain adopts a bilobal structure, in which the conserved catalytic cysteine residue lies within the C-terminal lobe, while the N-terminal lobe harbors the binding domain for E2 enzymes, mainly UbcH5 and UbcH7 (Schwarz et al., 1998). HECT domains are classified into 3 subgroups based on N-terminal architecture: the Nedd4 family, which contains WW domains (9 proteins), the HERC (HECT and RCC1-like domain) family containing RCC1-like domain (RLDs, 6 proteins), and other HECTs lacking either RLDs or WW domains (13 proteins) (Scheffner and Staub, 2007; Rotin and Kumar, 2009). In addition to the HECT domain, they have protein-protein interaction domains

for target recognition and/or localization in the N-terminal region, such as SH3, RING-finger, or coiled-coil domains.

Huwe1, a HECT domain E3 ubiquitin ligase

The HECT-domain E3 ubiquitin ligase Huwe1 (HECT, UBA, and WWE domain containing 1) is a large protein of 4371 amino acids. Huwe1 is involved in the assembly of K48 polyubiquitin chain for proteasomal degradation of several substrates, including polymerase γ (Markkanen et al., 2012), an anti-apoptotic protein Mcl-1 (Zhong et al., 2005; Kurokawa et al., 2013), BRCA1 (Wang et al., 2013), proto-oncoproteins, c-Myc and n-Myc (Adhikary et al., 2005; Zhao et al., 2008; Inoue et al., 2013), Myc-associated protein Miz1 (Yang et al., 2010b; Inoue et al., 2013), transcription factor MyoD (Noy et al., 2012), dishevelled (de Groot et al., 2014), and histone deacetylase HDAC2 (Zhang et al., 2011). Most of the substrate control is through K48 polyubiquitin chains for proteasomal degradation. However, Huwe1 also has non-proteolytic functions by forming K63-linked polyubiquitin chains for c-Myc (Adhikary et al., 2005) and both K63 and K11-linked polyubiquitin chains for dishevelled (Dvl), a cytoplasmic Wnt pathway component (de Groot et al., 2014).

Huwe1 is involved in tumor formation. Overexpression of Huwe1 has been observed in breast, lung and colon cancer (Adhikary et al., 2005; Chen et al., 2005), due to its substrates' functions in cell proliferation, apoptosis and DNA repair. For example, Huwe1 may cause genomic instability and oncogenic transformation, leading to tumorigenesis through its effects on tumor suppressor genes p53, BRCA1 and Mcl-1 (Chen et al., 2005; Zhong et al., 2005; Wang et al., 2013). Its biological roles in development and neurogenesis are more recently described (Zhao et al., 2008; Zhao et al., 2009; D'Arca et al., 2010).

Degron

A degron is a sequence element or modification sufficient to be recognized or targeted by an E3 ligase to promote ubiquitylation (Varshavsky, 1991). Many RING and HECT domain E3 ligases recognize substrates through "phosphodegrons," phosphorylated residues that mark proteins for ubiquitylation and degradation (Skowyra et al., 1997) (Ye et al., 2004; Gao et al., 2011a; Inuzuka et al., 2012). β-catenin is marked for ubiquitylation (mediated by ubiquitin ligase, Skp1-cullin1-Fbox- β-Trcp) and proteasomal degradation (Latres et al., 1999; Wu et al., 2003) by a two-step, sequential phosphorylation, primed by casein kinase 1α (CK1α) followed by glycogen synthase kinase 3 (GSK3), generating the phosphorylated sequence, DpSGIHpS. Other post-translational modifications, including hydroxylation (Ivan et al., 2001; Jaakkola et al., 2001), and methylation (Lee et al., 2012), have also been reported to signal for ubiquitylation.

Ubiquitin-proteasome as a regulator of transcription factors

Over six hundred E3 ligases control expression levels of transcription factors with important roles in development and regeneration. Cells utilize spatial distribution of E3 ligases to regulate local abundance of proteins and compartmentalization of different subcellular domains within the cells. They also employ the ubiquitin-proteasome system to control transcription factor availability at each stage of development or regeneration. The control of timing and level of transcription factors provided by proteasomal degradation is thought to be essential for the precise timing of development and regeneration in addition to their control by transcriptional regulatory cascades.

As an example, β-catenin regulation by the ubiquitin-proteasome pathway is crucial for its function in cell differentiation (Hirabayashi et al., 2004; Tsuchiya et al., 2007; Shi et al., 2010; Kondo et al., 2011), proliferation (Shi et al., 2012) and self-renewal (Barker et al., 2007; Qyang et al., 2007). In the absence of Wnt signaling, ß-catenin is phosphorylated by a degradation complex consisting of degron-forming kinases, GSK3 and CK1α, as well as adenomatous polyposis coli (APC), leading to proteasomal degradation through K48-ubiquitylation by Skp1-cullin1-Fbox- β-Trcp E3 ligase (Clevers, 2006). Binding of Wnt receptor Frizzled activates the Dvl cytoplasmic phosphoproteins and inhibits GSK3 and the related destruction complex, blocking the proteasomal degradation of β–catenin. y Maintaining β-catenin at a baseline level appears to be a mechanism to keep a cell poised to respond to Wnt signaling. β-catenin plays important roles in cochlear development: it drives cell division and upregulates Atoh1 in the differentiation of hair cells (Shi et al., 2010; Shi et al., 2014).

Chapter 2: Regulation of Atoh1 by the ubiquitin-proteasome pathway

Summary

The ubiquitin-proteasome pathway regulates the level of transcription factors during development and in regenerative responses. Here we show that Atoh1 is a short-lived protein degraded through the ubiquitin-proteasome pathway, as evidenced by extension of the half-life of Atoh1 by proteasome inhibitors and by identification of lysine 48-linked polyubiquitin chains on Atoh1 as a targeting mechanism for proteasomal degradation. We also find that amino acids 306-347 in the C-terminus of Atoh1 account for its stability. Cross-species sequence comparison shows that five serine residues in the C-terminus are conserved across species, and serine 334 is a key residue in the designation of Atoh1 for proteasomal degradation.

Results

Atoh1 is a short-lived protein

To determine the half-life of Atoh1, we used cycloheximide to prevent new protein synthesis and followed the time course of disappearance of previously synthesized Atoh1 by Western blotting during a chase period. We stably transfected 293T cells with *FLAG-HA-Atoh1* and treated with cycloheximide at 24 hours after plating of cells.

Pre-existing Atoh1 protein was completely degraded by 2 hours after inhibition of new protein synthesis. The half-life, as measured by densitometry in three experiments was 35.31 minutes (95% confidence interval: 24.11 +/- 65.97 minutes; Figure 2-1).

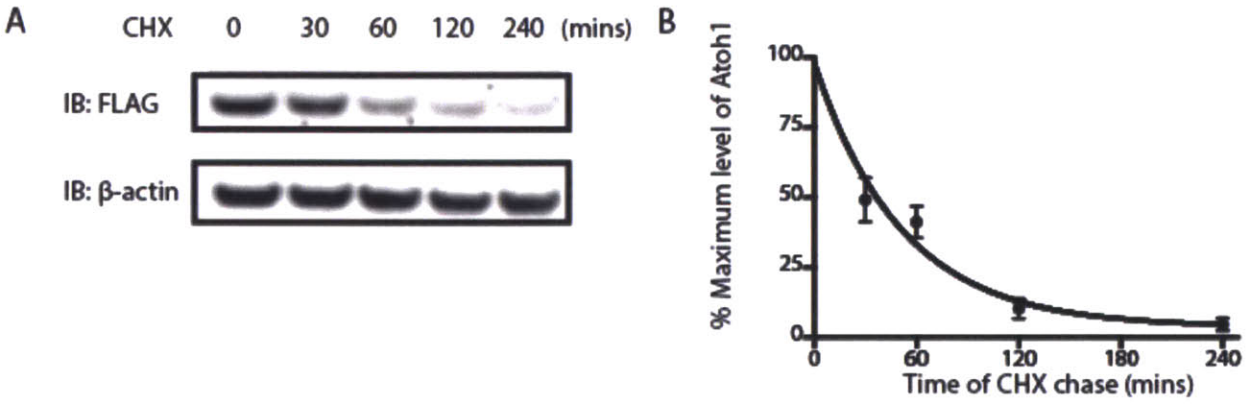

Figure 2- 1. Atoh1 is a short-lived protein
(A) Determination of the half-life of Atoh1. *FLAG-HA-Atoh1* 293T cells were treated with cycloheximide (CHX) (100 μg/ml) and harvested at the indicated times. Lysates were processed for Western blotting with FLAG antibody (Atoh1) or β-actin antibody (loading control). Labels indicate the time of chase.
(B) Protein half-lives based on densitometry. The ratio of Atoh1 to β-actin was plotted after normalizing to the initial ratio set to 100. Error bars indicate SEM.

Atoh1 is degraded by the ubiquitin-proteasome pathway

Since Atoh1 is a highly unstable protein with a turnover rate of less than 1 hour, we assessed the mechanism of degradation. When treated with MG132, a potent proteasome inhibitor, the level of Atoh1 was significantly increased (Figure 2-2A), suggesting that inhibition spared Atoh1 from proteasomal degradation. Proteasome inhibition extended the half-life of Atoh1 in a cycloheximide chase assay (Figure 2-2B & 2C), indicating that it interfered with Atoh1 degradation.

We then assessed polyubiquitylation of Atoh1 in the presence of a proteasome inhibitor. We prepared HEK cells stably transfected with *FLAG-HA-Atoh1* and treated with MG132 to inhibit proteasomal degradation. The cell lysates were immunoprecipitated with anti-FLAG antibody, and the pattern of ubiquitylation was assessed with an anti-ubiquitin antibody. Western blotting of immunoprecipitated FLAG-Atoh1 revealed high molecular weight forms of Atoh1, indicating polyubiquitylation (Figure 2-2D & 2E). Increased density of these high molecular weight forms was seen in samples treated with proteasome inhibitor, MG132, indicating accumulation of polyubiquitylated Atoh1.

To determine if Atoh1 formed K48-linked polyubiquitin, the form of polyubiquitin chain targeted for proteasomal degradation, we co-transfected HEK cells with *FLAG-Atoh1* and *ubiquitin* plasmid with mutations in all lysines except K48, or without mutations. The formation of high molecular weight bands above the Atoh1 bands on immunoblots suggested that K48 ubiquitin chains were formed on Atoh1 in both cases (Figure 2-3).

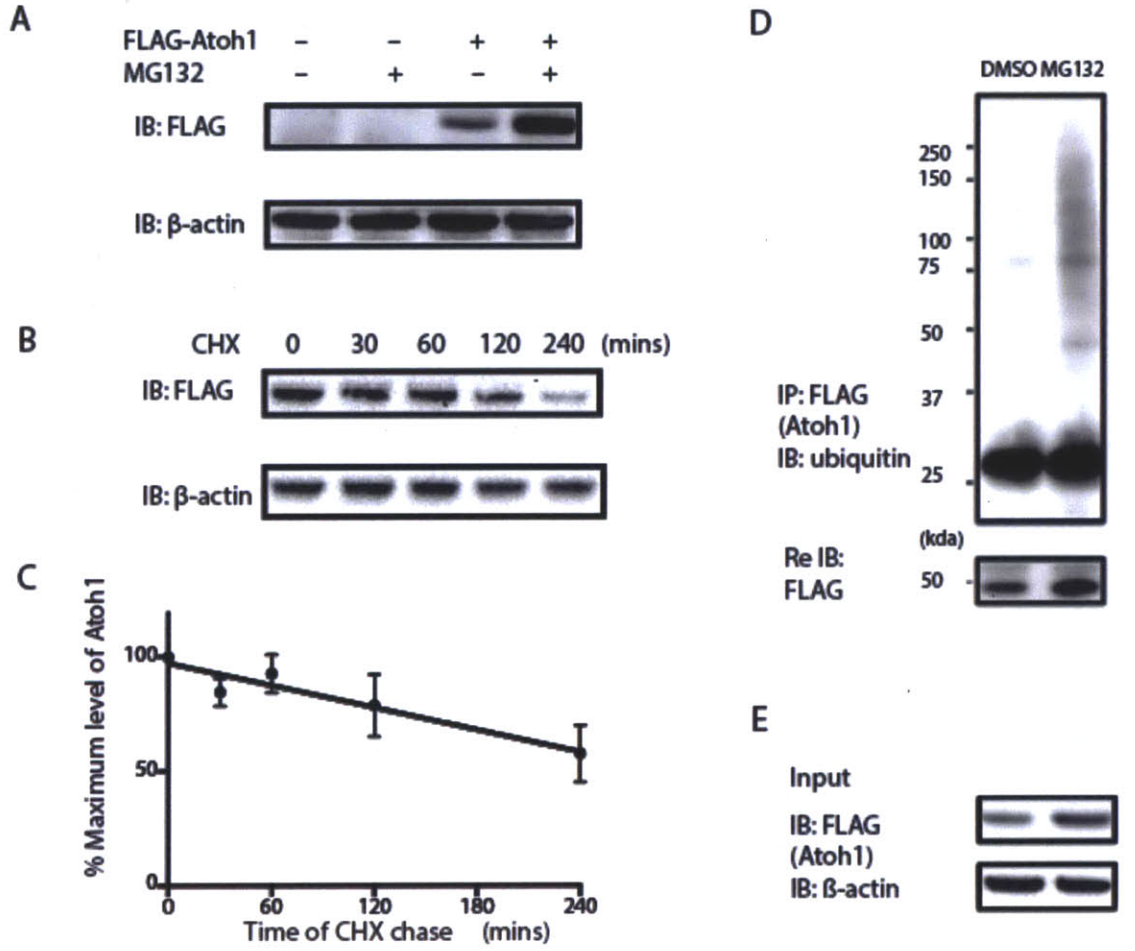

Figure 2-2. Atoh1 is degraded by the ubiquitin-proteasome pathway
(A) Proteasome inhibition stabilized Atoh1 expression in HEK cells. HEK cells were transfected with the *FLAG-Atoh1* plasmid (1 μg/ml) for 24 hours and incubated with either DMSO or MG132 (10 μM) for 3 hours, followed by immunoprecipitation with FLAG (Atoh1) or β-actin (loading control) antibodies.
(B) Determination of Atoh1 half-life with proteasome inhibition. *FLAG-HA-Atoh1* 293T cells were treated with MG132 (10 μM) at time 0 and cycloheximide (100 μg/ml) at the indicated times and immunoprecipitated with FLAG (Atoh1) or β-actin (loading control) antibodies. Time of treatment is indicated.
(C) Half-lives based on densitometry. The ratio of Atoh1 to β-actin was plotted after normalization. Error bars indicate SEM. Data from 3 experiments are shown.
(D) & (E). Atoh1 is polyubiquitylated and degraded by the ubiquitin-proteasome pathway. *FLAG-HA-Atoh1* 293T cells were treated with either DMSO or MG132 (10 μM) for 6 hours. Lysates were immunoprecipitated with anti-FLAG antibody and subjected to immunoblotting with a ubiquitin antibody. FLAG was used to assess immunoprecipitation. MG132 treatment increased the density of the poly-ubiquitin chains of Atoh1 and increased the level of protein as seen both by reprobing the blot and assessing the input protein (E). β-actin is a loading control.

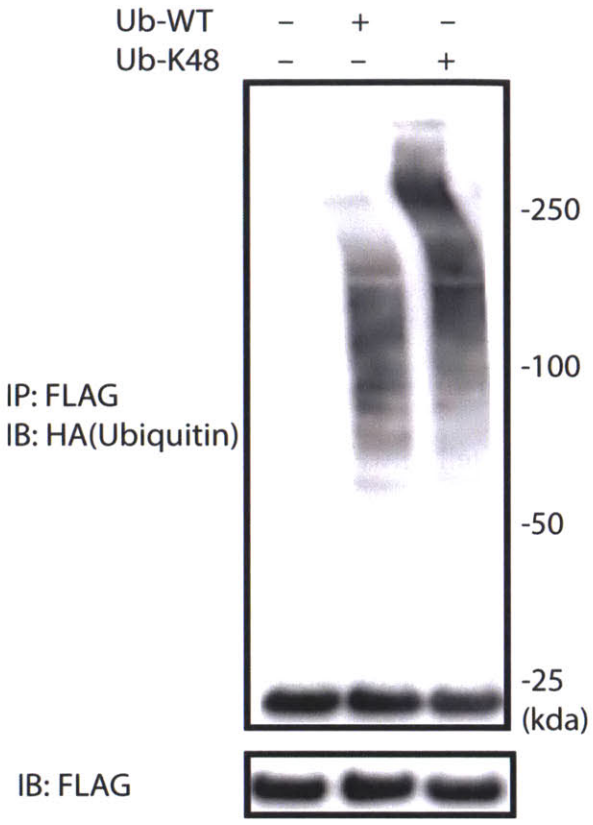

Figure 2-3. Atoh1 forms K48-linked polyubiquitin chains
Ubiquitylation by ubiquitin with mutated lysines. HEK 293T cells were co-transfected with *FLAG-Atoh1* and either wild-type *HA-ubiquitin* (WT) or *ubiquitin* with all lysines except K48 mutated, or empty vector. *FLAG-Atoh1* was immunoprecipitated and blotted with antibodies against HA (ubiquitin) and FLAG (Atoh1). FLAG antibody was used to confirm the immunoprecipitation of Atoh1.

Evolutionarily conserved serines in the C-terminus account for Atoh1 stability

We next generated a panel of two N-terminal (Δ10-93 for deletion 1 and Δ94-156 for deletion 2) and two C-terminal (Δ214-305 for deletion 3 and Δ306-347 deletion 4) deletions of *Atoh1* plasmids, retaining the bHLH domain (Figure 2-4A, right panel) to assess which regions might affect degradation. Atoh1-deletion 4 had the longest half-life in a cycloheximide chase assay, suggesting that motifs affecting the half-life of Atoh1 fell between amino acids 306 and 347 (Figure 2-4B).

Cross-species sequence comparison of *Atoh1* by MegaAlign (DNAstar, Madison, WI) indicated that serines 309, 325, 328, 331 and 334 were conserved across species (Figure 2-5A). Since conservation may relate to biological function, we generated mutated *Atoh1* plasmids containing alanine in the place of each serine. The S334A mutant was protected from degradation based on its higher level of expression and the lack of any further effect of proteasome inhibition with MG132, while wild-type and other mutants were affected (Figure 2-5B). Mutations at positions 328 and 331 modestly prolonged Atoh1 half-life, while mutation at position 334 had a dramatic effect (Figure 2-5C). We conclude that Ser 334 in the C-terminus of Atoh1 contains a motif that specifies Atoh1 for proteasomal degradation.

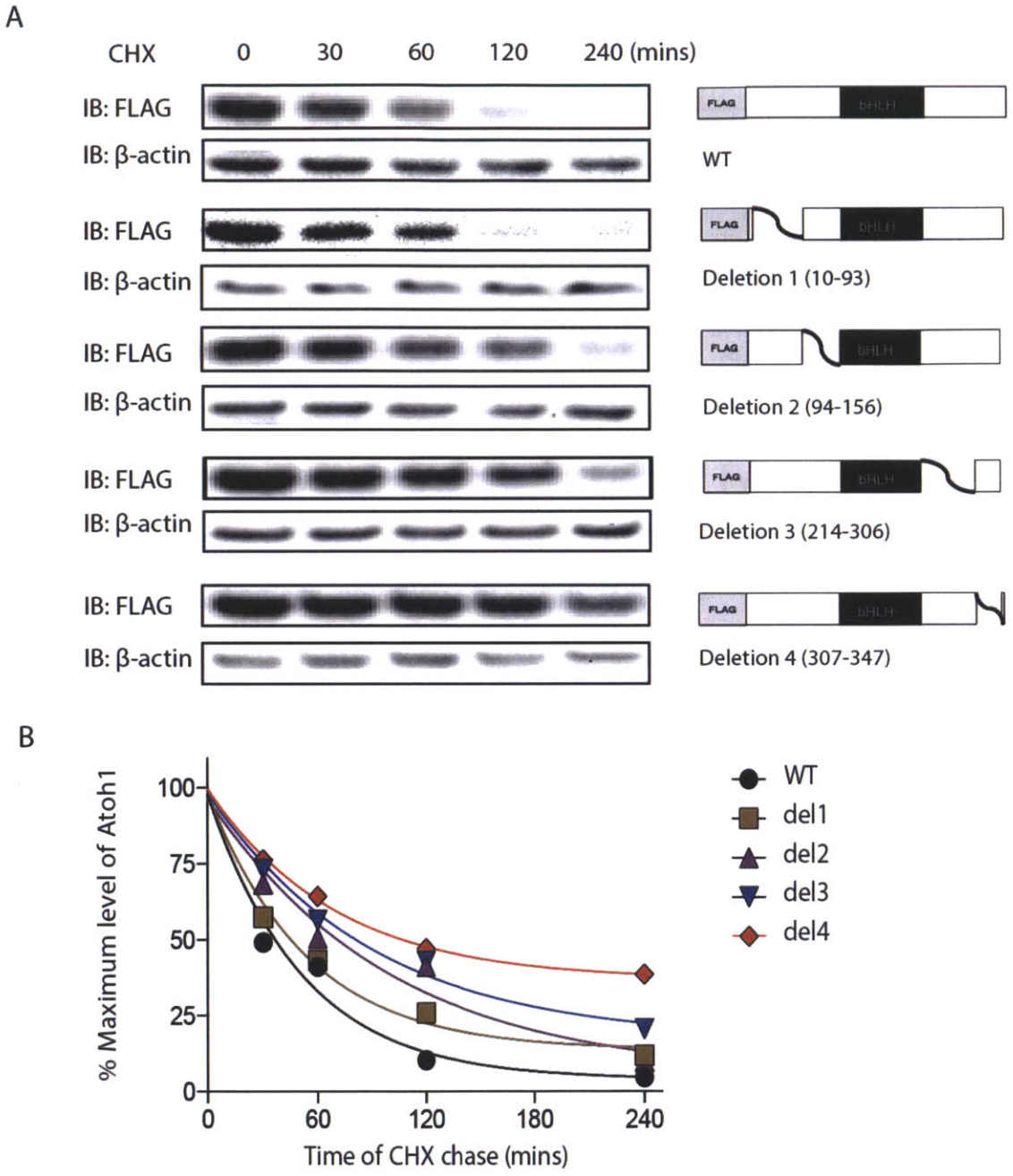

Figure 2- 4. Evolutionarily conserved serines in the C-terminus of Atoh1 account for its stability

(A) Half-life analysis of truncated Atoh1 over a 4-hour time frame. HEK cells were transfected with either wild-type or truncated *FLAG-Atoh1* for 48 hours and incubated with cycloheximide (100 μg/ml) for the indicated times. β-actin served as a loading control for input protein.
(B) Quantification of protein half-lives. The ratio of Atoh1 to β-actin based on densitometry was plotted.

A

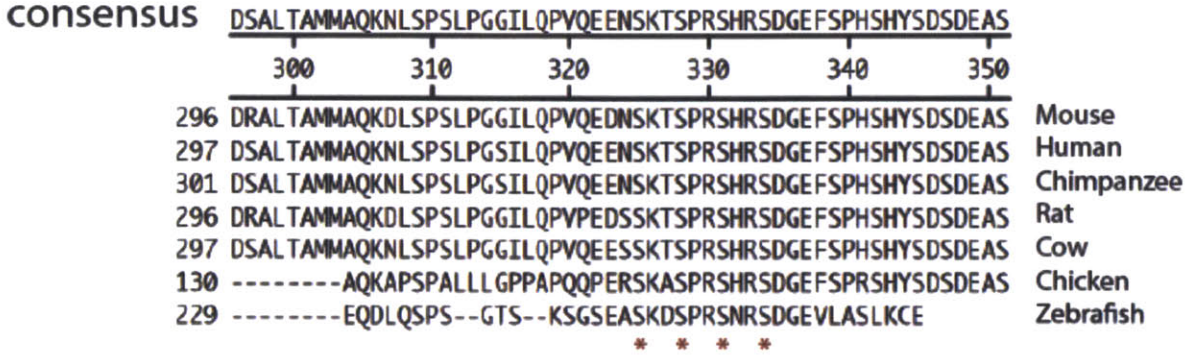
consensus DSALTAMMAQKNLSPSLPGGILQPVQEENSKTSPRSHRSDGEFSPHSHYSDSDEAS
300 310 320 330 340 350
296 DRALTAMMAQKDLSPSLPGGILQPVQEDNSKTSPRSHRSDGEFSPHSHYSDSDEAS Mouse
297 DSALTAMMAQKNLSPSLPGSILQPVQEENSKTSPRSHRSDGEFSPHSHYSDSDEAS Human
301 DSALTAMMAQKNLSPSLPGSILQPVQEENSKTSPRSHRSDGEFSPHSHYSDSDEAS Chimpanzee
296 DRALTAMMAQKDLSPSLPGGILQPVPEDSSKTSPRSHRSDGEFSPHSHYSDSDEAS Rat
297 DSALTAMMAQKNLSPSLPGGILQPVQEESSKTSPRSHRSDGEFSPHSHYSDSDEAS Cow
130 --------AQKAPSPALLLGPPAPQQPERSKASPRSHRSDGEFSPRSHYSDSDEAS Chicken
229 --------EQDLQSPS--GTS--KSGSEASKDSPRSNRSDGEVLASLKCE Zebrafish
* * * *

B

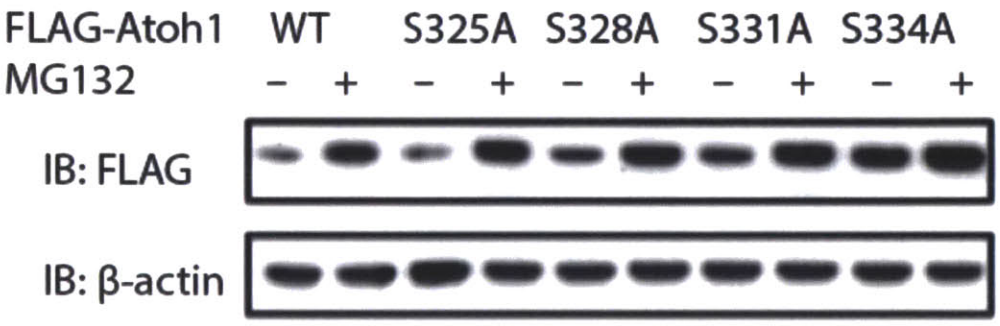
FLAG-Atoh1 WT S325A S328A S331A S334A
MG132 − + − + − + − + − +
IB: FLAG
IB: β-actin

C

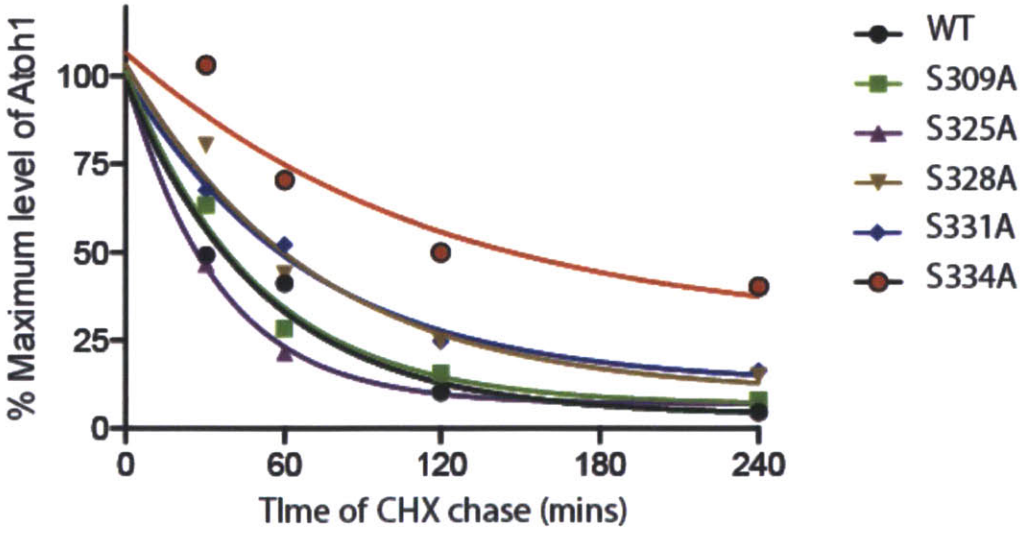
% Maximum level of Atoh1
100
75
50
25
0
0 60 120 180 240
Time of CHX chase (mins)
WT
S309A
S325A
S328A
S331A
S334A

Figure 2-5. S334 is a critical residue for Atoh1 degradation
(A) C-terminal regions of Atoh1 (area 4) of different species were aligned. Conserved serines at 325, 328, 331 and 334 are marked with asterisks.
(B) Serine to alanine mutations affect the steady-state level of Atoh1. HEK cells were transfected with wild-type or mutated *FLAG-Atoh1* plasmids for 40 hours and treated with either vehicle (DMSO) or MG132 (10 μM). After treatment with proteasome inhibitor for 6 hours, S334A had the smallest increase in Atoh1 (vehicle treatment is marked with a minus sign) compared to wild-type or other Atoh1 mutants.
(C) Half-life analysis of mutated Atoh1 proteins over a 4-hour time frame. HEK cells were transfected with either wild-type or mutated *FLAG-Atoh1* plasmids for 40 hours and incubated with cycloheximide (100 μg/ml) for the indicated times. The ratio of Atoh1 to β-actin based on densitometry was plotted.

S334 is involved in transcriptional activation of downstream genes

To further assess potential roles of the C-terminal segment in the metabolism of Atoh1, we performed dual luciferase reporter assays using a firefly reporter construct with an Atoh1 E-box associated motif (AtEAM) and a *Renilla* control reporter. AtEAM is a 10 amino acid Atoh1- specific binding motif that represents the site for activity of Atoh1 in numerous downstream genes (Klisch et al., 2011). We compared wild-type Atoh1 to the mutants made by serine to alanine changes at the 5 conserved serines of the Atoh1 C-terminus, S309, S325, S328, S331 and S334. Mutation of serine 334 to alanine caused a decreased signal ($p < 0.05$), indicating a role in downstream transcriptional activation (Figure 2-6). Thus in addition to increased degradation after phosphorylation of S334, it appears to play a role in the transcription of downstream targets of Atoh1.

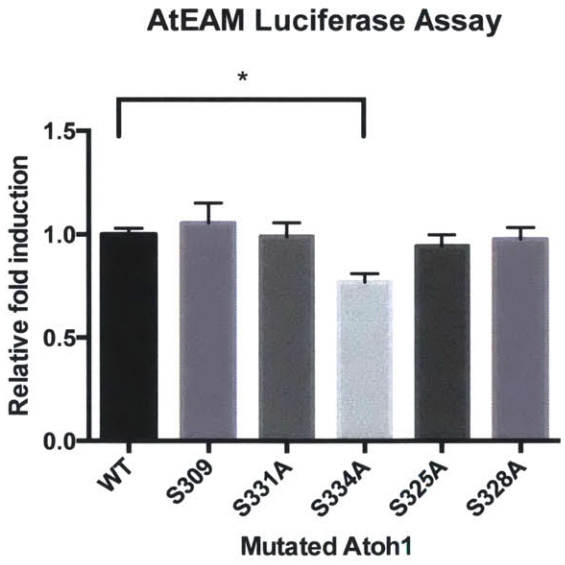

Figure 2-6. S334 decreased Atoh1 E-box reporter activity
Effect of serine to alanine mutation on Atoh1 signaling. Dual luciferase reporter assay using a firefly reporter construct with an AtEAM motif in HEK cells, co-transfected with either wild-type (WT) or mutated *FLAG-Atoh1* (S309A, S325A, S328A, S331A and S334A). Experiments were done in triplicate, and data are presented as the mean ± SEM after normalization to *Renilla* luciferase (*$p < 0.05$).

Discussion

Precise control of protein degradation underlies many fundamental cellular processes (Kawabe and Brose, 2011) (Tai and Schuman, 2008). Intracellular protein degradation may be achieved by autophagy or by the proteasome (Goldberg, 2003). The autophagy pathway is used for proteins with longer half-life, such as structural proteins, while proteins with a short half-life, especially transcription factors, are degraded through the ubiquitin-proteasome pathway.

Atoh1 is a critical transcription factor for the development of hair cells. We found that Atoh1 had a short half-life and was degraded through K48-linked ubiquitylation. We also identified sequence motifs related to degradation. A C-terminal region that was conserved across multiple species influenced Atoh1 stability. Having determined that a sequence responsible for Atoh1 stability lay between amino acids 306-347, we found that mutation of Ser 334 to Ala protected Atoh1, making this a promising site for post-translational modification leading to E3 ligase activity. Other proneural bHLH transcription factors are modified by phosphorylation or acetylation to generate degrons (Inuzuka et al., 2012, Gao et al., 2011, Hwang et al., 2010). Transcription factors Neurog1, Neurog2, NeuroD1 and Ascl1 contain conserved serine-rich sequences in this region (figure), and, in some cases, these have been shown to be responsible for protein stability (Khoo et al., 2003, Dufton et al., 2005, Li et al., 2012, McDowell et al., 2014).

Interestingly, the same mutation also decreased downstream transcriptional activation, as shown by lower activity of the AtEAM reporter in the S334A mutant, raising the possibility that Ser 334 was responsible for both degradation and transcriptional activation. Several transcription factors have degrons within transcriptional activation domains, including bHLH transcription factors Myc, Myf5, HIF-1a, MITF, Neurog2 and NeuroD1 (Geng et al., 2012, Khoo et al., 2003, Li et al., 2012). Even when the degron was deleted or mutated to increase the abundance of the protein, lower downstream transcriptional activity was observed (Guo et al.,

2009, Li et al., 2012, Khoo et al., 2003), suggesting a mechanistic connection between transcriptional activation and the ubiquitin-proteasome pathway. So far, no satisfying model can fully explain why two seemingly opposing biological functions, transcriptional activation and proteasomal degradation, are linked, and the mechanism underlying the extended half-life but decreased transcriptional activity of the S334A mutant of Atoh1 requires further investigation.

Despite our discovery that proteasome inhibition stabilized Atoh1, understanding the E3 ligase targeting Atoh1 is important since proteasome inhibitors provide little specificity. Inhibition of the E3 ligase could be very selective, and, since ubiquitylation follows the binding of E3 ligase, we assessed the degron-E3 ligase interaction and ubiquitylation to identify the degron responsible for Atoh1 degradation. In the next chapter, we identify E3 ligases that bind to the degron, and we discuss candidates for the putative kinases.

Materials and Methods

Cell culture

HEK cells, *FLAG-HA-Atoh1* 293T cells and HeLa cells were grown in DMEM supplemented with 10% heat-inactivated fetal bovine serum, 2 mM Glutamax and penicillin (100 U/ml)/streptomycin (100 μg /ml) (all from Invitrogen). All cultures were maintained in a 5% CO2/20% humidified incubator (Forma Scientific).

Generation of Atoh1 plasmids and stably expressing cell line

To generate *FLAG-Atoh1* plasmids, a construct consisting of *Atoh1* cDNA modified to include two consecutive *FLAG-tag* sequences (GATTACAAGGATGACGA) preceding the start codon, was subcloned into pcDNA3.1(+)(Parker et al., 2014).

Atoh1 mutants, including deletions (Δ10-93 for deletion 1, Δ94-105 for deletion 2, Δ214-305 for deletion 3 and Δ306-347 deletion 4) and mutations at the C-terminus (serine 309, 325, 328, 331 or 334 to alanine) were generated using the QuickChange Site-directed Mutagenesis Kit (Stratagene). All mutants were sequenced in their entirety.

To generate *FLAG-HA-Atoh1* plasmids, sequence-verified *Atoh1* clones in *pDONR223* were recombined into the Gateway destination vector *pHAGE-N-Flag-HA* (Invitrogen) using λ recombinase (Sowa et al., 2009). To generate lentivirus for the 293T cell line stably expressing *Atoh1*, 1 μg of *pHAGE-N-FLAG-HA-Atoh1* cDNA was co-transfected with 4 helper plasmids (2 μg of VSVG, 1 μg each of *Tat1b, Mgpm2*, and *CMV-Rev*) using Lipofectamine 2000 (Invitrogen) in 10 cm dishes of 293T cells. Virus particles were harvested 48 hours post-transfection and used to infect 293T cells. Puromycin (Sigma, 1 μg/ml) was used for the selection of infected cells (Sowa et al., 2009).

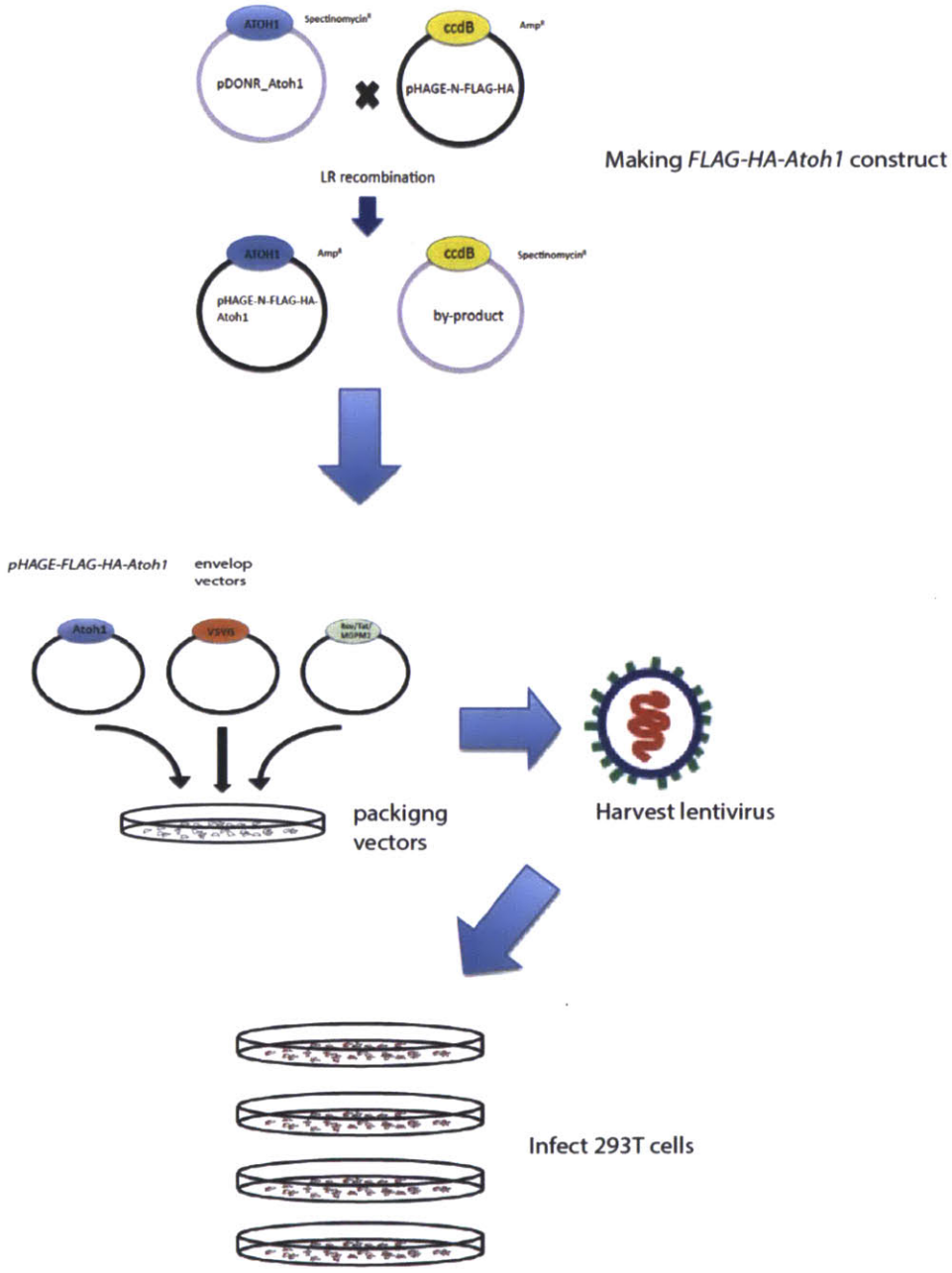

Figure 2-7. Generation of a *FLAG-HA-Atoh1* stably expressing cell line
A construct containing the transgene was incorporated into a lentiviral vector. After recombination of the *FLAG-HA-Atoh1* construct to place the transgene under the promoter, *FLAG-HA-Atoh1* along with the packaging plasmids were transfected into 293T cells. Lentivirus particles expressing *FLAG-HA-Atoh1* were harvested and infected into 293T cells again. Cells expressing the transgene were selected by growth in medium containing puromycin.

Western blotting

Proteins extracted with RIPA buffer from whole cells were separated on 4-12% NuPAGE Bis-Tris gels (Invitrogen) and electrotransferred to 0.2 μm nitrocellulose membranes (BioRad). The membranes were probed with mouse anti-FLAG (Sigma-Aldrich), mouse anti-HA (Sigma-Aldrich), mouse anti-ubiquitin (Santa Cruz), mouse anti-β-actin (Sigma-Aldrich), or mouse anti-HSC70 (1:10,000, Santa Cruz Biotechnology) antibodies, followed by HRP-conjugated, anti-rabbit or anti-mouse IgG, or anti-mouse light chain antibody (Jackson Immunoresearch Laboratories). The blots were processed with ECL or ECL-Plus Western Blot Substrates (Thermo). Band intensity was quantified by densitometry using Quantity One software (Bio-Rad). Each band was normalized to β-actin or HSC70 and expressed as a ratio to the control.

Cycloheximide chase assays for stability

HEK cells were transfected with either *FLAG-Atoh1* (wild-type), or indicated mutant *FLAG-Atoh1* plasmids (1 μg/ml) using Lipofectamine 2000 (3 μl per 1 μg of cDNA, Invitrogen). Forty-eight hours after transfection, 100 μg/ml cycloheximide (Sigma) was added to block protein synthesis. Cells were harvested at 0, 30, 60, 120, and 240 minutes. Equal amounts of protein from each treatment were taken for Western blotting. Protein bands were quantified by densitometry. The half-lives of indicated proteins were calculated using GraphPad Prism 6 software and a one-phase exponential-decay model. Each experiment was repeated at least two times.

Co-immunoprecipitation

To determine if the ubiquitin-proteasome pathway was involved in Atoh1 degradation, HEK cells were transfected with *FLAG-Atoh1* (1 μg/ml) using Lipofectamine 2000 (Invitrogen) for 48 hours and either DMSO or MG132 (10 μM) for 6 hours. Transfected cells were lysed in Pierce IP Lysis Buffer (Thermo) containing 1x complete protease inhibitors and 1x PhosSTOP phosphatase inhibitors (Roche). Lysates were immunoprecipitated with Anti-FLAG M2 Affinity Gel (Sigma-Aldrich) and immunoblotted by the procedures mentioned above.

To determine K48 polyubiquitylation, HEK cells were co-transfected with *FLAG-Atoh1* (1 μg/ml) and wild-type, K48 *ubiquitin* plasmids or empty vector (0.5 μg/ml, from Addgene) using Lipofectamine 2000 (Invitrogen). At 48 hours post-transfection, cells were lysed and immunoprecipitated with anti-FLAG M2 Affinity gel and immunoblotted.

Luciferase assay

10^5 HEK cells were seeded into a 96-well plate 1 day before transfection. 50 ng of firefly report construct with an Atoh1 E-box associated motif (AtEAM), 5 ng of Renilla-luciferase construct, and 50 ng of wild-type or mutated *Atoh1* plasmids were mixed 0.3 ul of Lipofectamine 2000 and incubated with the cells for 48 hours, until cells were lysed. Luciferase activity were measure by the Dual Luciferase Reporter Assay System (Promega) in a Victor3 plate reader (Perkin Elmer).

Statistical analysis

The means and standard errors of the mean were calculated and analyzed for significance by an unpaired two-tailed Student's t-test with indicated alpha (0.05) with Prism 6 software.

Chapter 3: Identifying an E3 ubiquitin ligase for Atoh1

Summary

E3 ubiquitin ligases regulate biological activities by their role as catalysts of ubiquitin transfer and conjugation to protein substrates. The HECT domain E3 ubiquitin ligases form thioester bonds with ubiquitin on an active site cysteine residue during the transfer of ubiquitin to substrates. Here we have used an immunoprecipitation/mass spectrometry screen to identify Huwe1, a HECT domain E3 ligase, as an Atoh1 binding partner. We validate the binding between Atoh1 and Huwe1 through reciprocal co-immunoprecipitation and mass spectrometry. We also find that Huwe1 promotes the polyubiquitylation of Atoh1 through a lysine 48-linked polyubiquitin chain and that mutation of the catalytic cysteine in the HECT domain of Huwe1 reduces the polyubiquitylation of Atoh1. Accordingly, overexpression of Huwe1 reduces the steady-state level of Atoh1 while Huwe1 knockdown by RNA interference stabilizes Atoh1. Finally, Huwe1 binds to an Atoh1 degron in the C-terminus, which contains evolutionally conserved serines, for polyubiquitylation, but doesn't bind to truncated Atoh1 that lacks this degron motif. We have thus defined a Huwe1-ubiquitin pathway that regulates Atoh1.

Results

Identifying Atoh1-interacting proteins by mass spectrometry

We performed immuoprecipitation followed by mass spectrometry (IP/MS) to identify binding partners of Atoh1 and searched the partners for E3 ubiquitin ligases that could be involved in the ubiquitin-proteasomal degradation (Sowa et al., 2009). We used a stably expressing 293T cell line prepared by lentiviral infection of *pHAGE-FLAG-HA-Atoh1*. Lysates of *FLAG-HA-Atoh1* 293T cells immunoprecipitated with HA antibody were subjected to LC-MS/MS analysis to identify proteins associated with Atoh1. We used *CompPASS*, an unbiased comparative approach for identifying high-confidence candidate interacting proteins, to interrogate datasets for parallel mass spectral studies (Sowa et al., 2009; Tan et al., 2013). The scoring metrics, WD^N, were used to assign scores to each protein. Proteins with a WD^N score greater one were considered high-confidence interacting partners (Table I).

E-proteins, E12 and E47 (TCF3 products), which are known interacting partners of Atoh1, were obtained in the high-confidence candidates and validated the IP/MS approach. Another E-protein, TCF12, which has not been reported to bind Atoh1, was also found as Atoh1 binding partner.

Two de-ubiquitinating enzymes, USP11 and USP47, were observed associated with Atoh1. These enzymes cleave the bond between ubiquitin and substrate protein. E3 ubiquitin ligase, Huwe1, was also observed in the high-confidence proteins and was the only ligase that passed the criteria for WD^N and Z scores among the Atoh1 interactors.

Table I

	Symbol	Gene ID	WD^N_Score
ATOH1	ATOH1	474	7.21
E3 ligase	**HUWE1**	10075	3.44
Ubiquitin-related enzymes	USP11	8237	1.41
	USP47	55031	2.00
E-protein	TCF3	6929	3.16
	TCF12	6938	2.00
Cell Death and Survival	AHSA1	10598	5.03
	ATP2A1	487	1.41
	MAPK3	5595	2.00
	PRDX4	10549	1.23
	PRPS1	5631	1.00
	SRI	6717	1.41
Cell movement	ENAH	55740	1.41
	FLNC	2318	1.15
	GFAP	2670	2.45
	PDE4D	5144	1.41
	SLC3A2	6520	1.41
	TUBA1C	84790	1.39
	TUBA4A	7277	3.00
	TUBB2B	347733	2.58
	ZYX	7791	1.58
OTHERS	AAMP	14	1.00
	ACOX1	51	1.72
	BCKDHA	593	2.00
	CCDC124	115098	1.00
	CPOX	1371	2.00
	CTPS2	56474	2.00
	EIF2C1	26523	1.00
	EIF2C2	27161	2.45
	EIF2C3	192669	1.00
	FHL3	2275	1.00
	NEK9	91754	2.83
	NT5DC2	64943	1.41
	PDXK	8566	1.41
	SEC23A	10484	1.23
	SEC23B	10483	1.00
	SERPINH1	871	1.00
	TNRC6C	57690	2.00
	YARS2	51067	1.41

Table I. Identifying Atoh1-interacting proteins by mass spectrometry
Lysates of *FLAG-HA-Atoh1* 293T cells were immunoprecipitated with HA antibody and subjected to proteomic analysis by LC-MS/MS. *CompPASS*, an unbiased comparative approach for identifying high-confidence candidate interacting proteins, was utilized to interrogate data sets and assign the WD^N scoring metrics. Proteins with a WD^N score greater than 1 fulfilled these criteria.

Immunoprecipitation confirms binding of Huwe1 to Atoh1

We first asked whether Huwe1 formed a physical complex with Atoh1 in HEK cells through reciprocal co-immunoprecipitation analyses (Figure 3-1). Mass spectrometric analysis of a Coomassie blue-stained band at 450 kDa from a lysate immunoprecipitated with an Atoh1 antibody identified Huwe1 as an interacting protein (Figure 3-1 and Table II). Mass spectrometry of the band at 45 kDa confirmed that the immunoprecipitated protein was FLAG-HA-Atoh1 (Table III).

Is Huwe1 an E3 ubiquitin ligase for Atoh1?

To determine whether Huwe1 can act as an E3 ubiquitin ligase for Atoh1, we performed an *in vivo* ubiquitylation assay. Increased ubiquitylation of Atoh1 was observed after transfecting *Huwe1* plasmids into *FLAG-HA-Atoh1* 293T cells, after co-immunoprecipitation, indicating a role of Huwe1 as an E3 ubiquitin ligase (Figure 3-2A). Furthermore, decreased poly-ubiquitylation was observed after Huwe1 knockdown, suggesting that E3 ubiquitin ligase activity on Atoh1 was inhibited. Similarly, increased polyubiquitylation, both wild-type and K48 ubiquitin chain, was seen in samples overexpressing Huwe1 (Figure 3-2B).

We also tested whether the ability of Huwe1 to transfer ubiquitin to Atoh1 was affected when a mutant form of *Huwe1* that had a serine in the place of a critical cysteine in the HECT domain (*Huwe1 C4341S*) (Herold et al., 2008; Zhao et al., 2008; Pandya et al., 2010) was used (Figure 3-3). The resulting decrease in both wild-type and K48 poly-ubiquitylated Atoh1 indicated that this active site residue was required for the ubiquitylation of Atoh1.

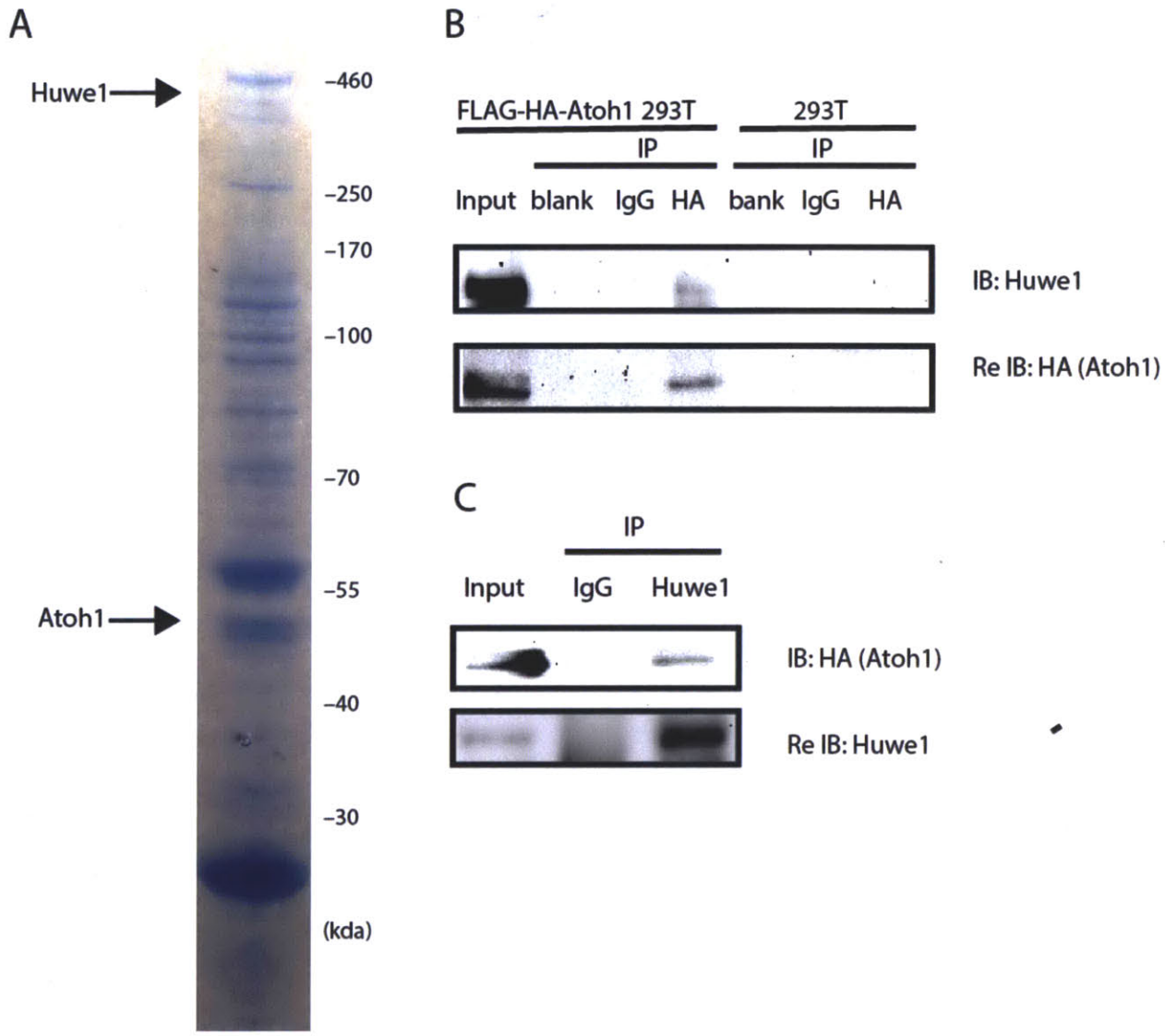

Figure 3- 1. Reciprocal immunoprecipitation confirmed the interaction of endogenous Huwe1 with Atoh1

(A) Coomassie blue staining of Atoh1-associated proteins. FLAG-HA tagged Atoh1 was purified from whole cell extracts of a stably transfected 293T cell line. Associated proteins were detected by Coomassie Blue staining. The areas indicated by the arrows were excised for mass spectrometry (Table II & III) and Western blotting.

(B) Co-immunoprecipitation of Huwe1 and Atoh1. *FLAG-HA-Atoh1* 293T lysates were immunoprecipitated with the indicated antibodies (IgG and HA) and subjected to immunoblotting with an antibody to Huwe1. The blot was stained with an HA antibody to confirm immunoprecipitation.

(C) Endogenous Huwe1 interacts with Atoh1. *FLAG-HA-Atoh1* 293T cell lysates were subjected to immunoprecipitation using IgG or Huwe1 antibody, followed by immunoblotting by HA antibodies to show the interaction with Atoh1 protein. Stripping and re-blotting with Huwe1 antibody was used to confirm immunoprecipitation.

Table II

Gene Symbol	Total peptide	Unique peptide	Average peptide score	Protein coverage
HUWE1	279	122	3.5367	28.78%
PRKDC	161	112	3.3479	25.48%
MAP1B	133	78	3.7349	37.68%
DYNC1H1	87	75	3.2275	18.02%
KIF11	79	46	3.3049	37.97%
SRRM2	53	38	3.7266	20.75%
MACF1	51	50	3.2235	8.57%
MYCBP2	51	47	3.3464	13.64%
MDN1	41	37	3.3880	8.79%
HERC2	36	34	3.2990	9.08%
RNF213	32	30	3.0488	6.38%
UBR5	31	26	3.3120	12.54%
UTRN	30	30	3.4022	10.81%
MGA	29	27	3.6467	13.52%
AKAP9	26	26	2.9820	8.08%
PRRC2C	26	21	3.2923	8.08%
CEP350	23	21	3.1575	11.08%
SON	22	20	3.6486	9.66%
PLEC	17	16	2.8815	3.86%
MAP1A	15	14	3.2701	8.46%
DMXL1	13	12	3.1873	5.48%
TRRAP	12	12	3.1620	3.91%
SACS	12	12	2.5812	2.88%
GOLGB1	12	10	2.8166	3.28%

Table II. Mass spectrometric analysis of suspected Huwe1
Coomassie Blue stained bands of 450 kda indicated in Figure 3-1 were excised and subjected to mass spectrometric analysis to validate Huwe1 as a binding partner of Atoh1.

Table III

Gene symbol	Total peptide	Unique peptide	Average peptide score	Protein coverage
TUBB2A	159	40	3.0903	55.51%
ATOH1	155	19	2.1144	34.18%
TUBA1A	112	34	3.1383	66.08%
RPL4	106	36	2.4767	53.63%
EEF1A1	103	28	2.6454	58.87%
TUFM	72	38	3.2781	68.36%
RPL3	67	29	2.5399	45.66%
SSB	65	30	2.8608	5.43%
RBMX	65	27	2.5009	47.06%
ENO1	62	34	3.1674	58.29%
PSMC5	52	31	3.5295	64.29%
PSMC2	50	29	2.9925	63.74%
YARS2	11	8	3.3677	29.77%
TUBA1C	7	11	3.6062	15.14%
SERPINH1	9	7	2.5123	20.81%
CSNK1D	7	4	3.1615	12.5%
CSNK1E	6	3	2.8233	9.86%
ACOX1	5	4	2.8799	10.30%
BCKDHA	5	3	2.6629	9.44%
PRPS1	3	3	2.6642	18.46%
TUBB2B	2	1	3.0318	2.70%
TUBA4A	1	1	3.4258	31.31%
PRDX4	1	1	3.1432	7.01%
AAMP	1	1	2.3377	2.53%
PDE4B	1	1	2.2331	2.04%

Table III. Mass spectrometric analysis to confirm immunoprecipitation of Atoh1
Coomassie blue stained bands of 45kda indicated in Figure 3-1 were excised and subjected to mass spectrometric analysis to validate immuoprecipitation of Atoh1.

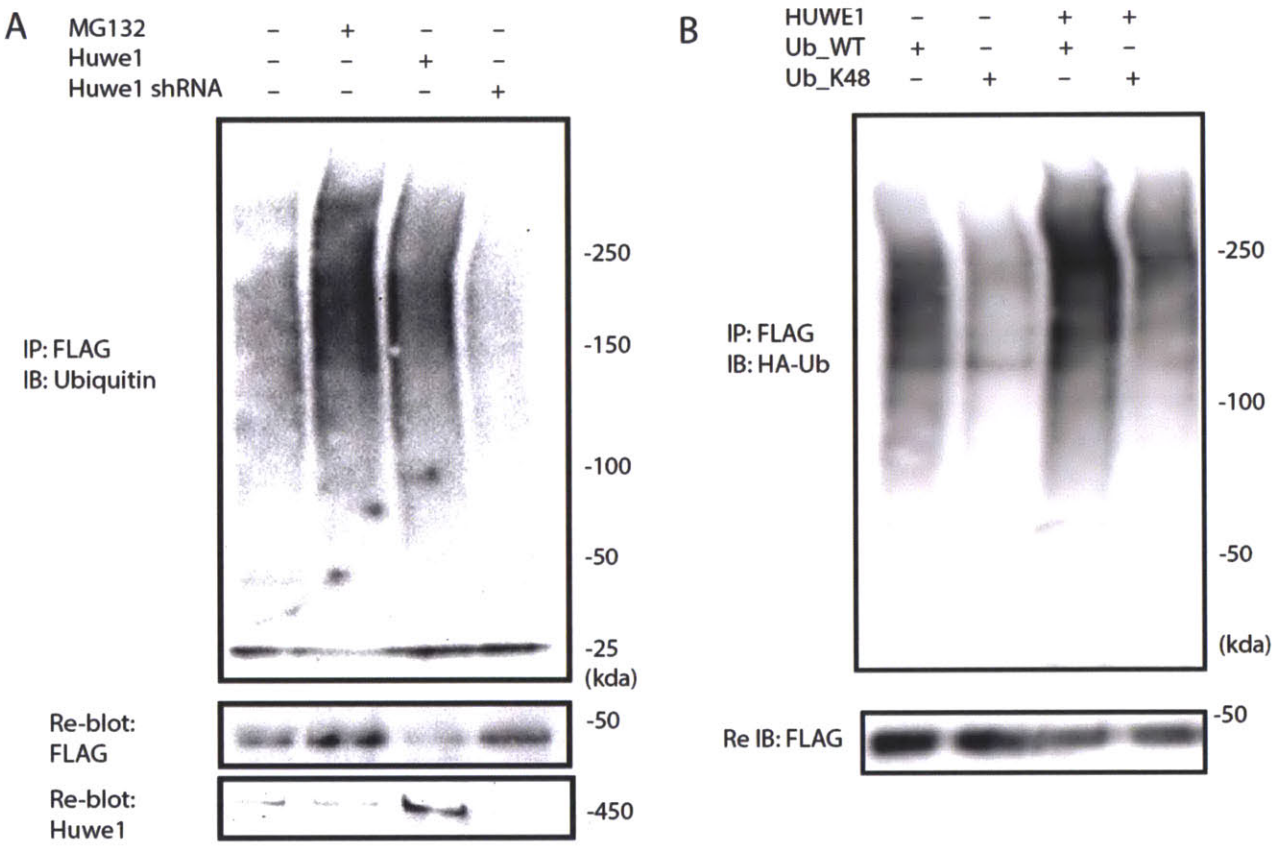

Figure 3- 2. Ubiquitylation of Atoh1 by Huwe1 occurs at K48
(A) Influence of Huwe1 on Atoh1 ubiquitin chains. *FLAG-HA-Atoh1* cells were transfected with empty vector, *Huwe1*, or *Huwe1* shRNA for 72 hours, and lysates were immunoprecipitated with antibodies against FLAG; lysates treated with MG132 for 4 hours before harvest serve as a positive control. An anti-ubiquitin antibody was used to detect ubiquitin conjugates; blots were stripped and reblotted with FLAG and Huwe1 antibodies. The lowest panel shows total extracts immunoblotted with an anti-FLAG antibody to detect FLAG-tagged Atoh1.
(B) Role of K48 ubiquitin chains. 293T cells co-transfected with empty vector or *Huwe1* and wild-type *HA-ubiquitin* (Ub_WT) or mutant lysine 48 (UB_K48) plasmids for 72 hours were lysed and subjected to immunoprecipitation with an anti-FLAG antibody. Ubiquitin conjugates were detected with an anti-HA antibody. The lower panel shows blots stripped and re-blotted with an anti-FLAG antibody.

A

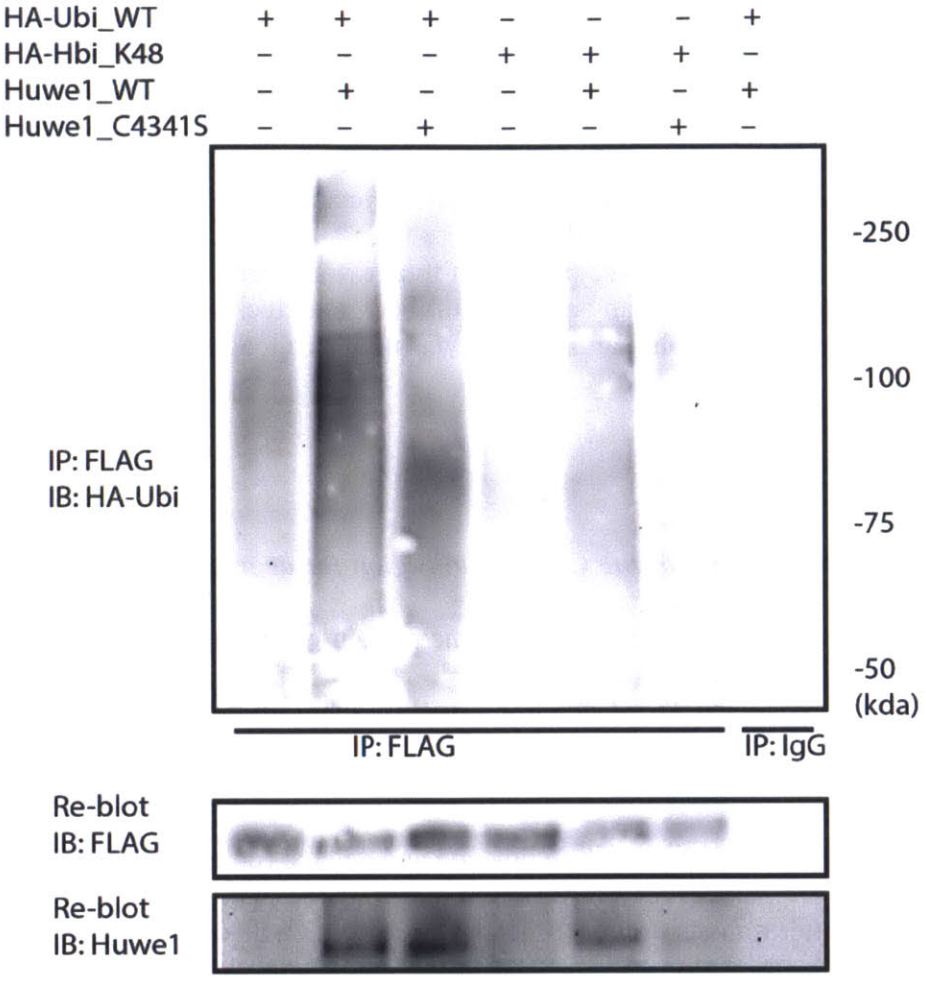
HA-Ubi_WT + + + − − − +
HA-Hbi_K48 − − − + + + −
Huwe1_WT − + − − + − +
Huwe1_C4341S − − + − − + −
-250
-100
-75
-50
(kda)
IP: FLAG
IB: HA-Ubi
IP: FLAG
IP: IgG
Re-blot
IB: FLAG
Re-blot
IB: Huwe1

B

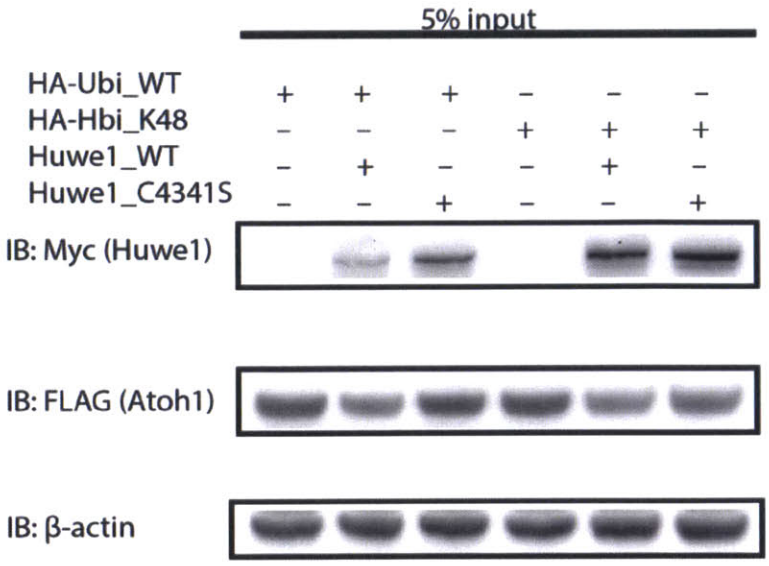
5% input
HA-Ubi_WT + + + − − −
HA-Hbi_K48 − − − + + +
Huwe1_WT − + − − + −
Huwe1_C4341S − − + − − +
IB: Myc (Huwe1)
IB: FLAG (Atoh1)
IB: β-actin

Figure 3- 3. Cysteine at position 4341 of Huwe1 is critical for ubiquitin transfer to Atoh1
(A) Wild-type, but not *C4341A*-mutant *Huwe1*, promotes polyubiquitylation of Atoh1. HeLa cells were co-transfected with *FLAG-Atoh1*, *HA-ubiquitin* (WT) or mutant lysine 48 only (K48), and *Myc-Huwe1* WT or *C4341A* plasmids. FLAG-Atoh1 was immunoprecipitated under denaturing conditions using anti-FLAG antibody, and polyubiquitylation of Atoh1 and total Atoh1 level were detected by Western blotting with anti-HA and anti-FLAG antibodies. Exogenous Huwe1 level was determined with an anti-Myc antibody. The lysates were immunoprecipitated with IgG as a control.
(B) Blotting of Huwe1 and Atoh1. Five percent of total extracts from the experiment shown in A were analyzed by Western blot with an anti-Myc antibody to detect exogenous Huwe1 and an anti-FLAG antibody to detect Atoh1; anti-β-actin was used as a loading control.

Confirmation of the importance of the C-terminal region for degradation

To determine whether specific regions of the protein were required for Huwe1 binding and ubiquitylation, we analyzed Atoh1 deletion mutants. Ubiquitylation (Figure 3-4A, bottom), as well as Huwe1 interaction (Figure 3-4A, top), were normal for the 3 of the deletion mutants when we co-transfected *Myc-Huwe1* with wild-type and deleted (deletions 1-3) *FLAG-Atoh1* plasmids, but absent after transfection of truncated Atoh1 with a deletion between amino acid 306-347 (deletion 4). This shows that the protein without the C-terminal region neither binds to Huwe1 nor forms polyubiquitin chains, confirming that this region was required and suggesting that a signal for degradation (a degron motif) resided in this location.

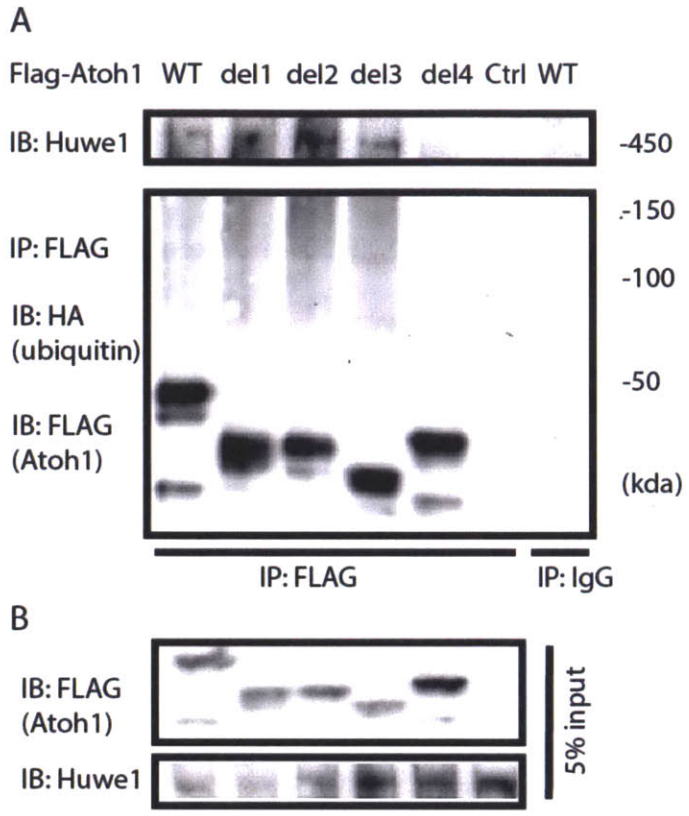

Figure 3- 4. A signal for Huwe1 binding is located in the C-terminus of Atoh1
(A) Truncation of Atoh1 influences Huwe1 interaction. HEK cells were co-transfected with *HA-ubiquitin* and wild-type or truncated *FLAG-Atoh1* plasmids (Δ10-93 for deletion 1, Δ94-156 for deletion 2, Δ214-305 for deletion 3 and Δ306-347 for deletion 4) for 48 hours. Immunoprecipitation was performed under denaturing conditions with anti-FLAG antibody. Atoh1 was detected with anti-HA and anti-FLAG antibodies. Endogenous Huwe1 was detected with an anti-Huwe1 antibody. Immunoprecipitation with IgG was used for the control.
(B) Blotting of endogenous Huwe 1 and Atoh1. Five percent of total extracts from the experiment shown in A were analyzed by Western blotting with an anti-FLAG antibody to detect Atoh1 and anti-Huwe1 to detect endogenous Huwe1.

Huwe1 knockdown extends the half-life of Atoh1

To determine whether Huwe1 affected the stability of Atoh1, *FLAG-HA-Atoh1* 293T cells were transfected with *Huwe1* plasmids or *Huwe1* shRNA for gain- or loss-of-function experiments respectively. *Huwe1* overexpression reduced Atoh1, while *Huwe1* knockdown stabilized Atoh1 (Figure 3-5, A & B).

The half-life of Atoh1 measured by a cycloheximide-chase assay also revealed that Huwe1 shRNA extended the half-life of Atoh1 in *FLAG-HA-Atoh1* 293T cells (Figure 3-5, C & D). These results support the hypothesis that Huwe1 degrades Atoh1 through the ubiquitin-proteasome pathway.

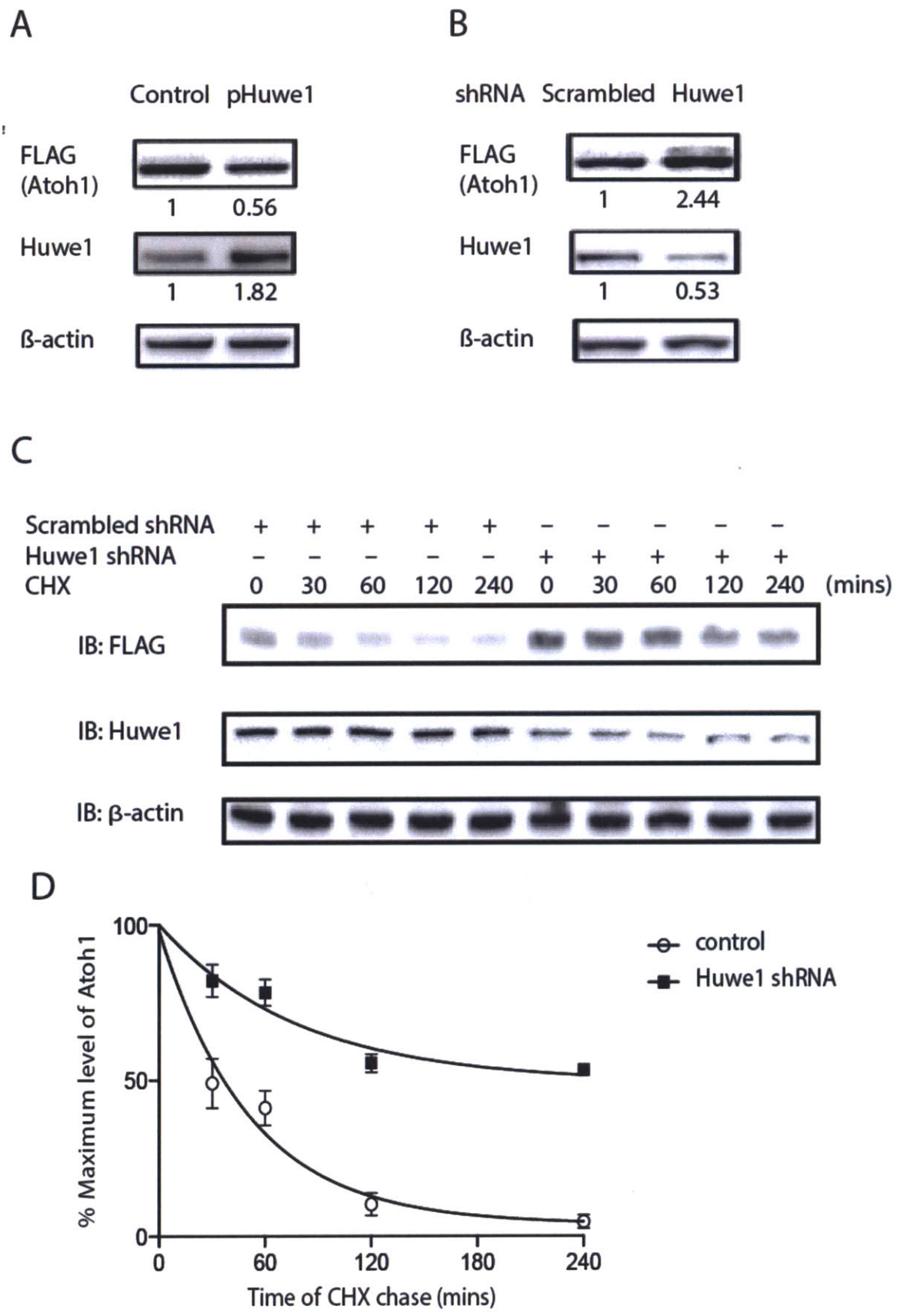
A
Control
pHuwe1
FLAG (Atoh1)
1
0.56
Huwe1
1
1.82
ß-actin
B
shRNA
Scrambled
Huwe1
FLAG (Atoh1)
1
2.44
Huwe1
1
0.53
ß-actin
C
Scrambled shRNA + + + + + − − − − −
Huwe1 shRNA − − − − − + + + + +
CHX 0 30 60 120 240 0 30 60 120 240 (mins)
IB: FLAG
IB: Huwe1
IB: β-actin
D
% Maximum level of Atoh1
100
50
0
0
60
120
180
240
Time of CHX chase (mins)
control
Huwe1 shRNA

Figure 3- 5. Huwe1 plasmid increased and Huwe1 shRNA inhibited degradation of Atoh1
(A) Co-transfection of Huwe1 and Atoh1. *FLAG-HA-Atoh1* 293T cells were transfected with *Huwe1* (1 μg/ml) for 48 hours. Quantification of Atoh1, Huwe1 and a loading control (HSC70) were performed by Western blotting and densitometry.
(B) Inhibition of Huwe1 expression with shRNA (100 nM) to Huwe1. *FLAG-HA-Atoh1* 293T cells were transfected with *Huwe1* shRNA for 72 hours.
(C) & (D). The half-life of Atoh1 was increased by *Huwe1* knockdown. *FLAG-HA-Atoh1* 293T cells were transfected with either control or *Huwe1* shRNA for 72 hours, and treated with cycloheximide (CHX, 100 μM) for the indicated times. Atoh1 (FLAG) and Huwe1 were analyzed by Western blotting and densitometry normalized to loading controls in three experiments. The ratio of Atoh1 to β-actin was plotted. Error bars indicate SEM.

Discussion

We identified Huwe1 as an Atoh1 ubiquitin ligase. Huwe1 conjugated Atoh1 with K48 ubiquitin chains. Truncated Atoh1 (deleted between amino acid 307 and 347) did not bind to Huwe1 and was not ubiquitylated. Consistent with a longer half-life (described previously in chapter 2), the degron for Atoh1 was in the C-terminus, as the C-terminus was necessary for recognition by Huwe1 and proteasomal degradation.

Huwe1 is a HECT domain E3 ubiquitin ligase. The HECT domain of Huwe1 is the catalytic domain, containing a conserved cysteine at position 4341 that forms an intermediate thioester bond with ubiquitin before transferring ubiquitin to substrate (Rotin and Kumar, 2009). Mutation of Cys 4341 to Ser or Ala reduces ubiquitin transfer through K11, K48 or K63 (Chen et al., 2005, Zhao et al., 2009, Pandya et al., 2010, Herold et al., 2008). The HECT domain does not affect substrate binding; that function is located in the N-terminus (Wang et al., 2013). Huwe1 C4341S showed reduced K48 ubiquitin conjugation to Atoh1. Polyubiquitylated Atoh1 was still detected in transfected lysates, however, suggesting that endogenous Huwe1 contributed to polyubiquitylation of Atoh1; the existence of other E3 ubiquitin ligases cannot be ruled out. C4341S Huwe1 had a decreased ability to conjugate ubiquitin but still bound to Atoh1.

Huwe1 is responsible for the stability of several transcription factors, including n-Myc (Zhao et al., 2008), c-Myc (Inoue et al., 2013), p53 (Chen et al., 2005), Mcl-1 (Zhong et al., 2005), Cdc6 (Hall et al., 2007), MyoD (Noy et al., 2012), and BRCA1 (Wang et al., 2013). However, in addition to degradation, Huwe1 polyubiquitylates several proteins through non-K48 linkages. For example, Huwe1 ubiquitylates Dvl through K11 and K63 linkage, whereby it inhibits multimerization of Dvl and Wnt signaling (de Groot et al., 2014). Huwe1 promotes

interaction of c-Myc with P300 and transcriptional activation via K63 ubiquitylation (Adhikary et al., 2005).

In addition to E3 ubiquitin ligase, substrate specificity also comes from post-translational modification of degrons, which allows substrate ubiquitylation in response to endogenous or external signals (Ravid and Hochstrasser, 2008). We found that the serine-enriched C-terminus of Atoh1 had putative motifs for phosphorylation by casein kinase 1 (CK1), pSer/Thr-X-X-Ser/Thr, starting from Ser 325, followed by Ser 328, 331 and 334. CK1 is a serine/threonine protein kinase that triggers phosphorylation of substrates, and has Ck1α, CK1δ, CK1ε and CK1γ isoforms. Since CK1 isoforms have molecular weight ranging from 32 to 52.5 kDa (Knippschild et al., 2014), which are close to Atoh1, we conducted mass spectrometry on the band at 45 kDa from lysates immunoprecipitated with Atoh1 (Table III). CK1ε and CK1γ were identified in the proteins at this molecular weight. Our preliminary data also showed that CK1 inhibitors, both IC-261 and PF-670462, increased the steady-state abundance of Atoh1 in the 293T cell line (data not shown). Further validation of the involvement of CK1 in degron phosphorylation and E3 ligase binding of Atoh1 will lead to a better understanding of the Atoh1-ubiquitin-Huwe1 pathway.

Interestingly, in addition to Huwe1, several other E3 ligases were also found as interacting proteins by mass spectrometric analysis of a Commassie Blue-stained band at 450 kDa from a lysate co-immunoprecipitated with Atoh1. These included Mycbp2, Herc2, RNF213, and Ubr5 (Figure 3-1 and Table III). Although none of the proteins pass the criteria of our initial immunoprecipitation-mass spectrometry screening (WD^N score over 1.0 by *CompPASS*), we cannot rule out roles as E3 ubiquitin ligases for Atoh1. Further validation of their interaction with Atoh1 would be needed to determine a role.

Materials and Methods

Protein purification

HEK293T cells with stable expression of Atoh1 from 15-cm tissue culture dishes at approximately 80% confluence were lysed in a total volume of 4 ml of lysis buffer (50 mM Tris pH 7.8, 150 mM sodium chloride, 0.5% NP40 plus EDTA-free protease inhibitor cocktail (Roche) and incubated at 4° C for 45 minutes. Lysates were centrifuged at 13,000 rpm for 10 minutes at 4° C and filtered through 0.45 μm spin filters (Millipore) to remove cell debris. Sixty μl of immobilized anti-HA resin (Sigma; 50% slurry) were used to immunoprecipitate the cleared lysates by gentle inversion overnight. Once the binding was complete, resin containing immuno-complex was washed with lysis buffer 4 times, followed by PBS 4 times. Atoh1 was eluted with HA peptide (250 μg/ml) in PBS for 30 minutes (3 X 50 μl) at room temperature. Ten percent of the eluate was electrophoresed on a NuPAGE Novex 4-12% Bis-Tris gel and silver stained to confirm immunoprecipitation of Atoh1 and the remaining eluate was subjected to trichloroacetic acid (TCA) precipitation for subsequent IP-MS/MS analysis.

In other experiments, specific bands stained for Commassie blue after elution were excised for peptide mass spectrometric sequencing at the core facility of Harvard Medical School.

Mass spectrometry

For identification of Atoh1 interacting proteins, the TCA-precipitated protein pellet was re-suspended in 25 μg/μl of sequencing grade trypsin (25 μg/μl in 30 μl 100 mM ammonium bicarbonate pH 8.0 with 10% acetonitrile) and incubated at 37° C for 4 hours. Digested samples were loaded onto stagetips and washed. Peptides were eluted with 50% formic acid/5%

acetonitrile to neutralize the trypsin, followed by drying and re-suspension in 10 µl of 5% formic acid/5% acetonitrile. The resulting spectra were analyzed by SEQUEST[1] against a human database(Eng et al., 1994). The list of proteins was loaded into *CompPASS* for further processing and analysis (Sowa et al., 2009).

Co-immunoprecipitation

FLAG-HA-Atoh1 293T were lysed with IP buffer and the lysates were immunoprecipitated with HA-resin (Sigma), IgG conjugated A/G agarose, or empty A/G agarose (Santa Cruz Biotechnology) and immunoblotted with antibodies against HA and Huwe1. For reciprocal immunoprecipitation, similar lysates were immunoprecipitated with A/G agarose conjugated with rabbit anti-Huwe1 antibody (Novus Biological) and immunoblotted with antibodies against HA or Huwe1.

To explore the role of Huwe1 on ubiquitylation of Atoh1, we generated *Myc-Huwe1* with cysteine 4341 mutated to alanine (*Myc-Huwe1-C4341*) by recombining Huwe1 pENTR plasmids (Addgene) into *pDEST-CMV-N-Myc* using Gateway cloning. *FLAG-HA-Atoh1* 293T cells were transfected with wild-type *Huwe1*, *Huwe1* shRNA (Sigma) or empty vector for 48 hours and treated with MG132 (10 µM) or vehicle for 6 hours. Cell lysates were immunoprecipitated with anti-FLAG-resin (Sigma) and immunoblotted with mouse anti-ubiquitin antibody (Santa Cruz Biotechnology) or reblotted with mouse anti-FLAG or rabbit anti-Huwe1 antibodies.

Wild-type or mutant *Myc-Huwe1*, wild-type or K48 *HA-ubiquitin*, and *FLAG-Atoh1* plasmids were co-transfected into HeLa cells. After 48 hours, cell lysates were immunoprecipitated with anti-FLAG resin and immunoblotted with mouse anti-HA, mouse anti-

[1] SEQUEST is a tandem mas spectrometry data analysis program for peptide sequencing and protein identification (Eng et al. 1994).

FLAG and rabbit anti-Huwe1 antibodies. Input was blotted with mouse anti-Myc, mouse anti-FLAG, and mouse anti-β-actin antibodies as loading controls.

Chapter 4: Hair cell differentiation after Huwe1 knockdown in the cochlea

Summary

Overexpression of proneural basic-helix-loop-helix transcription factor, Atoh1, induces ectopic hair cells and knockout prevents hair cell differentiation in the inner ear. From the data in cultured cell lines showing that overexpression of Huwe1 leads to downregulation of steady-state Atoh1 level while depletion of Huwe1 stabilizes Atoh1, we have concluded that Atoh1 is regulated by proteasomal degradation mediated by Huwe1. Here, we show that proteasome inhibition, as well as Huwe1 depletion, stabilize Atoh1 in the inner ear. A direct effect of proteasomal stabilization of Atoh1 by Huwe1 depletion is seen in the newborn cochlea, where its inhibition results in the generation of new hair cells, with the largest effect in the apical regions. The new hair cells lack labeling by EdU, indicating that the increase in hair cell number is a result of direct transdifferentiation of supporting cells rather than cell division.

Results

Inhibition of proteasomal activity stabilizes cochlear Atoh1

To test whether proteasomal activity regulated Atoh1 in the cochlea we treated P1 organ of Corti explants with proteasome inhibitor, MG132 (10 μM). An increase in Atoh1 after treatment with MG132 indicated that it was stabilized (Figure 4-1).

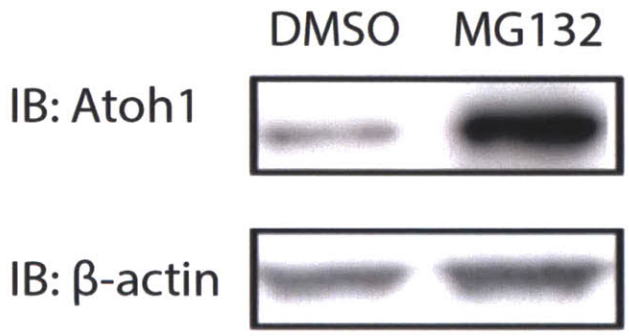

Figure 4-1. Inhibition of proteasome activity stabilizes Atoh1 in the cochlea
Treatment with the proteasome inhibitor. The organ of Corti from a P1 mouse was treated with proteasome inhibitor, MG132 (10 μM), for 3 hours. Atoh1 levels were higher in the MG132-treated organ of Corti. DMSO served as control; β-actin is a loading control.

Huwe1 knockdown increases Atoh1 in the organ of Corti

Treatment of organ of Corti explants from P1 mice with 100 nM *Huwe1* siRNA for 72 hours suppressed *Huwe1* gene expression by 59.5% as measured by real-time qRT-PCR (Figure 4-2) and decreased protein level by 55% on the basis of Western blot (Figure 4-3). Depletion of *Huwe1* with siRNA caused a marked accumulation of Atoh1 in the cochlea based on densitometry. Hair cell marker, myosin VIIa, was also upregulated by *Huwe1* siRNA, indicating a potential increase in the number of hair cells after stabilization of Atoh1 by knockdown of *Huwe1*.

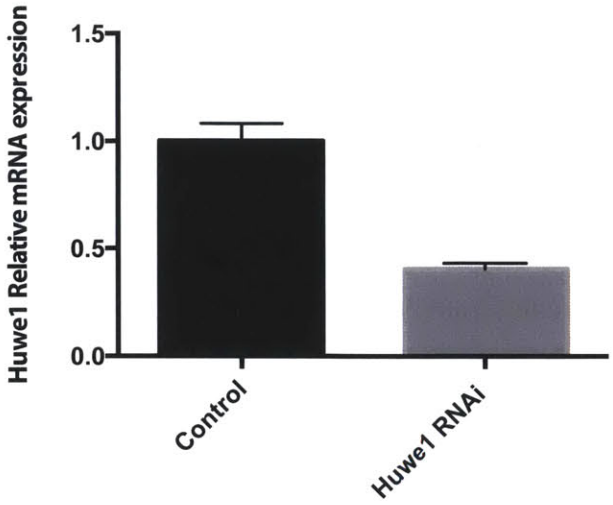

Figure 4-2. qRT-PCR of siRNA-treated organ of Corti
Quantification of *Huwe1* downregulation. P1 organ of Corti was treated with indicated siRNA (100 nM) for 72 hours. *Huwe1* siRNA suppressed *Huwe1* expression by 59.5%, compared to scrambled siRNA. Experiments were done in triplicate. Error bars indicate SEM.

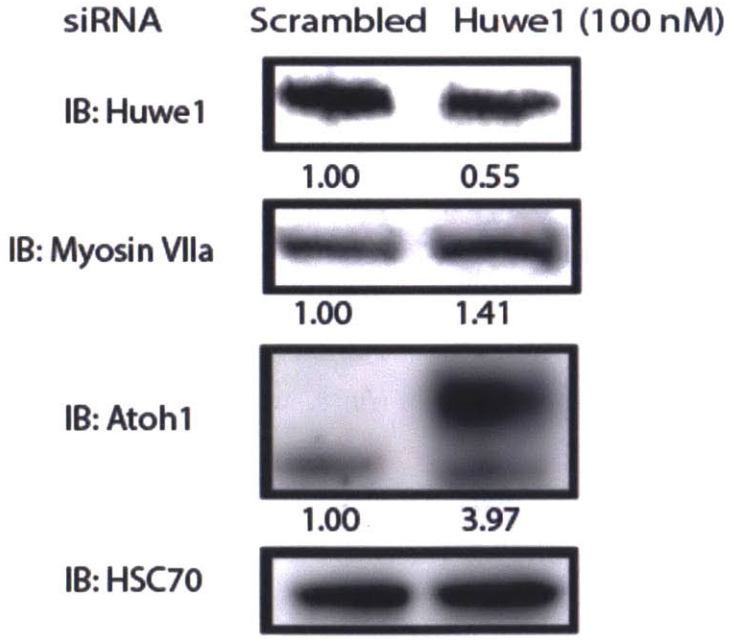

Figure 4-3. Huwe1 knockdown stabilizes Atoh1
Quantification of proteins after *Huwe1* siRNA. P1 organs of Corti were treated with the indicated siRNA (100 nM) for 72 hours. Huwe1, myosin VIIa and Atoh1 were quantified after Western blotting by densitometry and normalized to a loading control (HSC70).

Huwe1 knockdown increases hair cell generation in the organ of Corti

Since *Huwe1* knockdown stabilized Atoh1, we assessed its effect on hair cell generation in the cochlea. Treatment of organ of Corti explants with 100 nM *Huwe1* siRNA significantly increased the number of myosin VIIa-positive cells in the outer hair cell region (Figure 4-4A) (45.06 ± 2.10 vs 31.68 ± 2.66 after treatment with scrambled siRNA, $p<0.01$). *Huwe1* siRNA significantly increased hair cell formation in the apex (44.01±3.95 vs 31.48±3.85, $p<0.05$) and mid-apex (48.80±1.78 vs 31.43± 2.33, $p<0.001$) when the organ of Corti was quantified in four regions of equal length. Slight increases in the mid-base (44.76± 2.86 vs 40.81±3.08) and base (42.72±2.90 vs 38.26±4.13) were not significant (Figure 4-4B and 4C). The supernumerary hair cells showed hair cell bundle structures, as they were positive for phalloidin staining (Figure 4-4D).

New hair cells are not a result of proliferation

Supporting cells and hair cells were not labeled by 5-ethynyl-2'-deoxyuridine (EdU), a marker for cell division 72 hours after siRNA treatment of organ of Corti explants (Figure 4-5), indicating that they were not the product of renewed cell division of either cell type. The increase in hair cells generated by siRNA-mediated suppression of *Huwe1* was therefore a result of direct transdifferentiation of supporting cells.

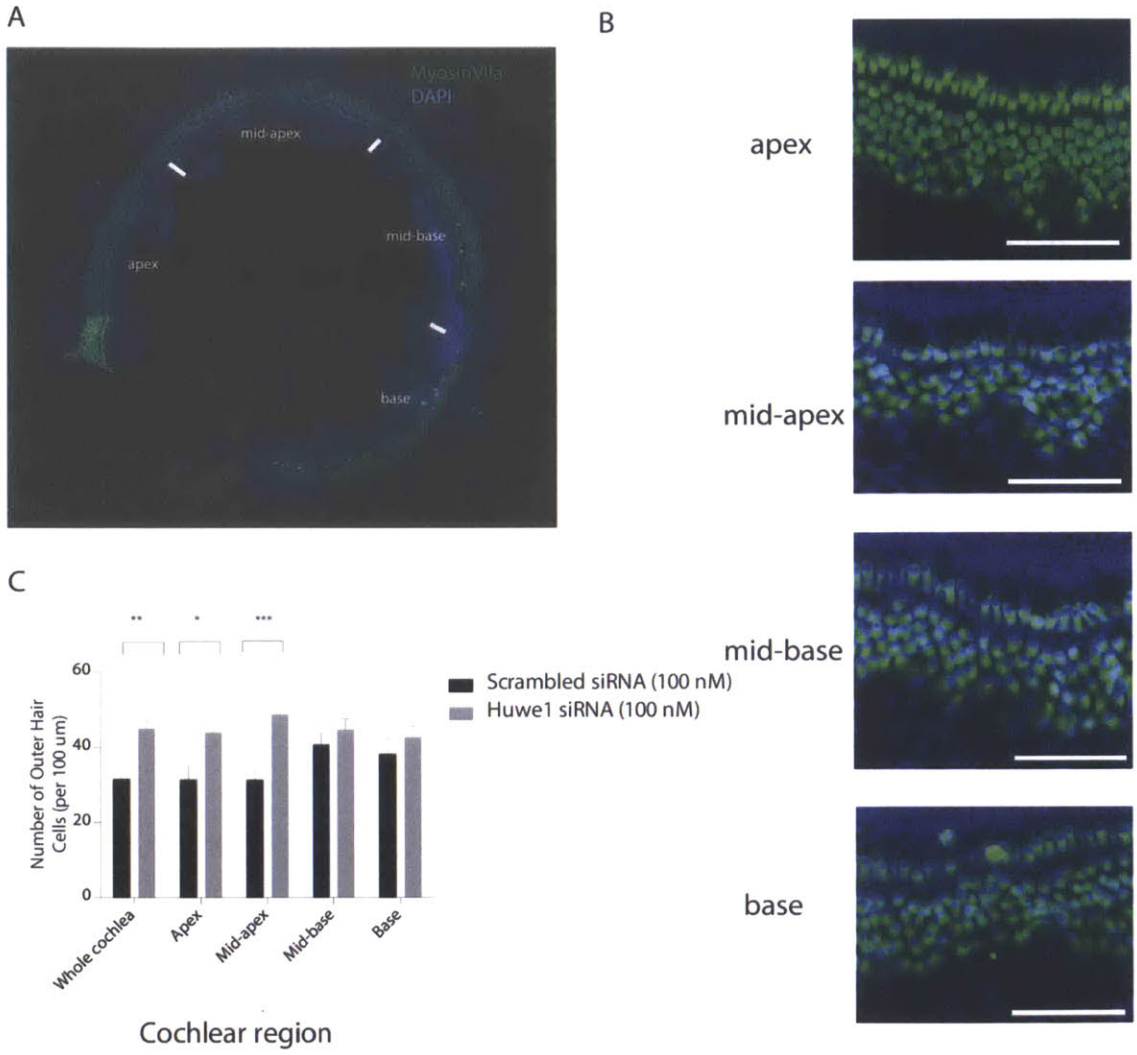
A
MyosinVIIa
DAPI
mid-apex
mid-base
apex
base
B
apex
mid-apex
mid-base
base
C
**
*
***
Number of Outer Hair Cells (per 100 um)
60
40
20
0
Scrambled siRNA (100 nM)
Huwe1 siRNA (100 nM)
Whole cochlea
Apex
Mid-apex
Mid-base
Base
Cochlear region
D
Merge
Phalloidin
MyosinVIIa
Scrambled siRNA-
Huwe1 siRNA

Figure 4-4. Huwe1 knockdown increases hair cell generation in organ of Corti explants
(A) & (B). Effect of Huwe1 knockdown on the organ of Corti. Organs of Corti treated with *Huwe1* siRNA (100 nM) for 72 hours have increased numbers of hair cells in the apex (0-25%), mid-apex (25-50%), mid-base (50-75%), and base (75-100%). The scale bar is 100 μm.
(C) Effect of Huwe1 knockdown was significant. Outer hair cell counts in the apex, mid-apex, mid-base, and base or the whole cochlea (mean ± SEM per 100 mm; *$p < 0.05$, **$p < 0.01$ ***$p<0.001$, n=7 for both groups).
(D) The supernumerary hair cells showed bundle structures. The increased hair cells from the organ of Corti treated with *Huwe1* siRNA (100 nM) for 72 hours were positive for phalloidin, a hair bundle marker. The scale bar is 100 μm.

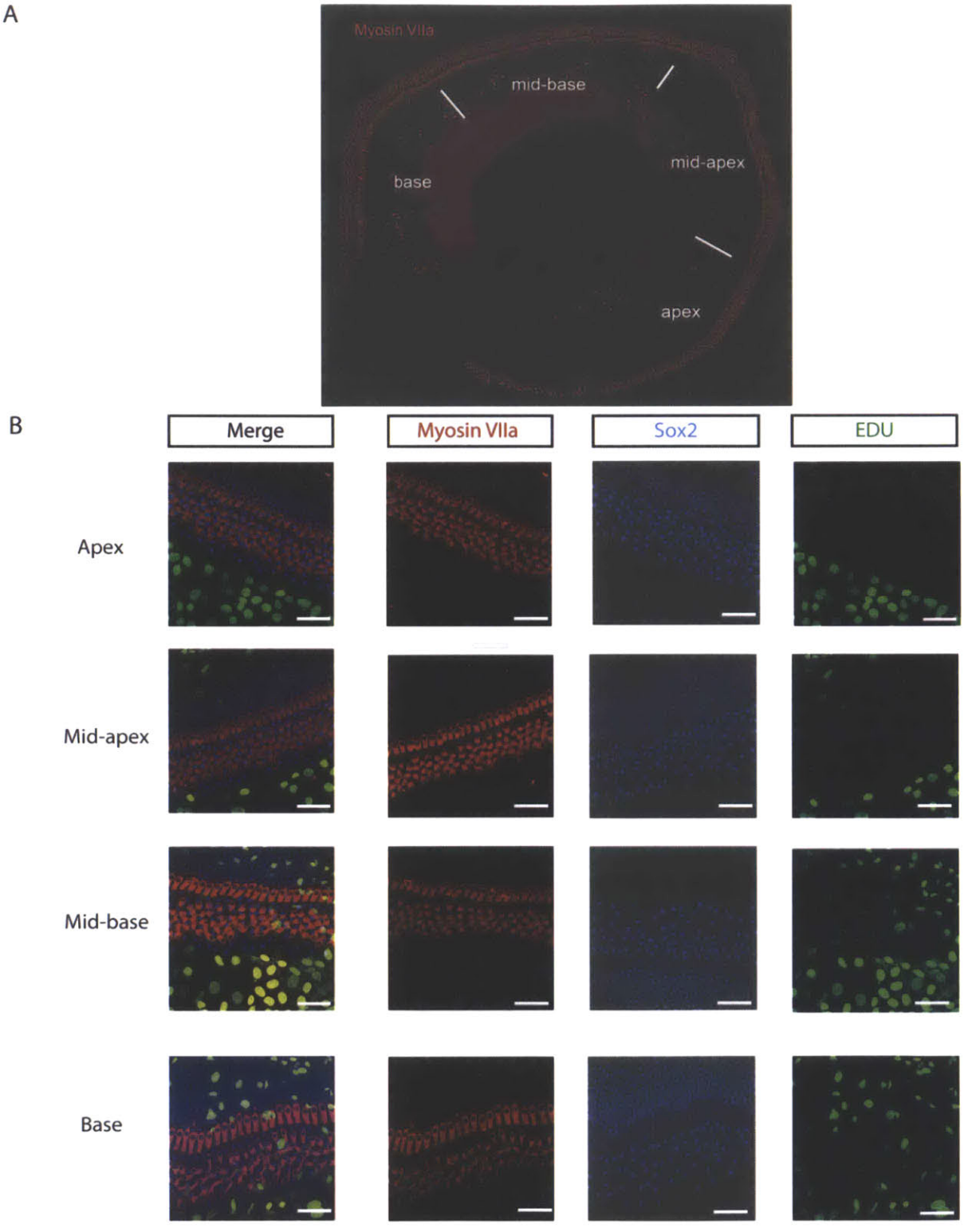
A
Myosin VIIa
mid-base
base
mid-apex
apex
B
Merge
Myosin VIIa
Sox2
EDU
Apex
Mid-apex
Mid-base
Base

Figure 4-5. Increased number of hair cells is not from proliferation
(A) Organ of Corti explant. Myosin VIIa-positive cells are seen throughout the organ of Corti explants.
(B) Effect of Huwe1 on supporting cell division and generation of hair cells. Organ of Corti explants treated with *Huwe1* siRNA for 72 hours showed an increase in myosin VIIa-positive cells. No co-staining for EdU-Sox2 or EdU-myosin VIIa was observed, indicating that supporting cells and hair cells had not divided (n=4). The scale bar is 100 μm.

Discussion

Atoh1 transcriptional regulation is complex and controlled by several pathways, such as Wnt (Shi et al., 2010), Sox2 (Neves et al., 2012), and Eya1-Six1 (Ahmed et al., 2012). Atoh1 binds to its own 3' enhancer and autoactivates the gene (Helms et al., 2000). Most of the transcriptional activators for *Atoh1* also bind at this enhancer. Because of its autoregulatory loop, *Atoh1* transcription is self-perpetuating. Whatever factors first activate *Atoh1* transcription have a powerful effect on its level, and regulators that can intervene in the loop are essential for maintaining Atoh1 at the appropriate level.

Transcription factors that counteract Atoh1, such as Hes and Id proteins (Kageyama et al., 2000, Bertrand et al., 2002, Imayoshi and Kageyama, 2014) are important in regulating its downstream activity, but the degradation mechanism of Atoh1 remains largely unknown. In this work, we shed light on this pathway by identification of its E3 ligase that controls Atoh1 stability.

We demonstrated that interfering with the ubiquitin-proteasome pathway, either by broadly-acting inhibition of proteasome activity or by specific knockdown of E3 ubiquitin ligase, stabilized Atoh1 in various cell lines. We found that the short-term application of proteasome inhibitor MG132 stabilized Atoh1 in the cochlea. However, due to the cytotoxicity of MG132, longer-term incubation caused apoptosis of cochlear cells (data not shown).

Proteasome inhibition influences cell division and apoptosis by affecting stabilization of many substrates (Teicher et al., 1999, Inuzuka et al., 2012, Voutsadakis, 2008). An effect on Atoh1 levels in the cochlea is expected to influence hair cell genesis because of the central role of Atoh1. In order to have better spatiotemporal control of protein abundance in hair cells, it is crucial to understand the mechanism underlying proteasomal degradation of Atoh1.

By identifying an E3 ubiquitin ligase specific to Atoh1, we were able to achieve more precise control of Atoh1 in the inner ear. *Huwe1* knockdown in the cochlea not only stabilized Atoh1, but also led to the generation of hair cells. Immunohistochemical results showed that Huwe1 knockdown increased the genesis of hair cells without causing proliferation of supporting cells. Thus the transdifferentiation of supporting cells was the mechanism for the increase in hair cell formation.

Huwe1 is responsible for the degradation of N-myc, and knockdown of Huwe1 increases proliferation of cortical progenitors (Zhao et al., 2008). In the inner ear, N-myc plays important roles in controlling proliferation, morphogenesis and patterning, and N-myc increased proliferation in chick otic vesicles (Domínguez-Frutos et al., 2011). Through incorporation of the proliferation marker EdU, we ruled out proliferation of supporting cells or hair cells as the source of increased hair cells, thereby excluding a direct contribution of N-myc stabilization. Several other transcription factors have been identified as Huwe1 substrates, and we cannot rule out a role of other substrates in the genesis of extra hair cells.

The increase in hair cell number after Atoh1 upregulation by Notch inhibition was apparent in the apex and middle region of the cochlea (Doetzlhofer et al., 2009, Mizutari et al., 2013, Bramhall et al., 2014). Huwe1 knockdown induced hair cell formation in the apex and mid-apex of the cochlea, while increases in hair cells in the mid-basal and basal regions were not obvious. These results reflect the general phenomenon of a relative immaturity of hair cells and more regenerative ability of supporting cells in the apex than in the base of the cochlea.

Materials and Methods

Neonatal cochlear explant culture

Cochlear tissues were dissected from 1-day postnatal CD-1 mice (Charles River Laboratories). Spiral ganglion, Reissner's membrane, and the hook region of the organ of Corti were removed to obtain a flat cochlear surface preparation(Parker et al., 2010). Explants were plated onto 4-well plates (Greiner Bio-One) coated with Matrigel (BD Biosciences) diluted 1:10 in DMEM supplemented with 10% fetal bovine serum overnight.

Huwe1 knockdown in the organ of Corti

As described previously, postnatal day 1 mouse organs of Corti were cultured on Matrigel-coated coverslips overnight. The organs were incubated with *Huwe1* or scrambled siRNA (IDT-DNA, 100 nM) for 72 hours.

Detection of proliferation by incorporation of 5-Ethynyl-2'-Deoxyuridine (EdU)

To evaluate cell proliferation, organs of Corti were incubated with 3 μM 5-ethynyl-2'-deoxyuridine (EdU) in combination with siRNA treatment and replenished after 36 hours. The tissue was fixed, blocked and permealized as described.

RNA preparation for quantitative RT-PCR

Total RNA was extracted with the RNeasy Mini Kit (Qiagen) according to the manufacturer's instructions. 1 μg RNA was reverse transcribed to cDNA using the Improm-II Reverse Transcription System (Promega). The reverse transcription conditions were 25° C for 10 min followed by 37° C for 60 min; the reaction was terminated at 95° C for 5 min. The cDNA

products were mixed with LightCycler Taqman Master Mix (Roche) and Taqman primers (Invitrogen) in a 96-well plate according to the manufacturer's instructions. The qPCR was run in triplicate on an ABI 7700 Real-Time PCR machine (Applied Biosystems, Inc.) with the initial denaturation at 95° C for 2 min, denaturation at 95° C for 15 s, and annealing/extension at 60° C for 1 min for 45 cycles. *Huwe1* gene expression was calculated relative to 18S RNA, and the amount of cDNA applied was adjusted to bring the Ct value for 18S RNA to within one half-cycle.

Antibodies used for Western blot

Western blot procedures were the same as described previously. Additional antibodies used were rabbit anti-Atoh1 (1:1,000, Affinity BioReagent Antibody), myosin VIIa antibody (1:200, Proteus Biomedical), and mouse anti-HSC70 (1:10,000, Santa Cruz Biotechnology).

Immunohistochemistry

Organ of Corti explants were fixed for 10 minutes in 4% paraformaldehyde, followed by three washes with PBS and blocking with 1% BSA and 5% goat serum in 0.1% Triton X-100 PBS (PBT1) for 1 hour. Explants were incubated overnight with PBT1, containing rabbit anti-myosin VIIa antibody (1:500, Proteus Biomedical), rabbit anti-Sox2 (1: 500, Santa Cruz Biotechnology). Samples were washed with PBS for 10 minutes and incubated with secondary antibodies conjugated with Alexa 488, 594 or 647 (Invitrogen). To visualize the organization of the actin filaments, the cells were incubated with 1:500 dilution of rhodamine phalloidin (Invitrogen) for 30 minutes and washed with PBS.

Detection of proliferation by incorporation of EdU

To evaluate cell proliferation, organ of Corti tissue was incubated with EdU in combination with siRNA treatment and replenished after 36 hours. The tissue was fixed, blocked and permeabilized as described. 70 µl of Alexa-Flour 488-conjugated azide cocktail (Invitrogen) was added to each well and incubated in a light-proof chamber at room temperature for 30 minutes. Tissues were washed with PBS before adding secondary antibodies.

Imaging and cell counting

Organs of Corti were analyzed using a Leica TCS SP5 confocal microscope. Inner and outer hair cells and supporting cells (in the outer hair cell region) were counted in cochlear whole mounts. High-power fluorescent images of the organ of Corti were merged in Adobe Illustrator CS6; total length and cell counts were determined with ImageJ software (NIH). Organs of Corti were divided into four regions (apex, mid-apex, mid-base, and base) and hair cell and supporting cells counts were obtained per 100 µm. Each counted segment was 1200-1400 µm.

Statistical analysis

The mean values and standard error of the mean were calculated and analyzed for significance by an unpaired two-tailed Student's t-test with indicated alpha (0.05, 0.01 or 0.001) with Prism 6 software.

Chapter 5. Conclusion and future directions

Summary

Inner ear development and regeneration rely not only on programmed gene expression and cell-cell signaling by molecules such as Notch and Wnt, but also on tightly-regulated control of protein level in both supporting cells and hair cells. The ubiquitin-proteasome pathway is an important mechanism controlling protein abundance. A key protein whose level is regulated spatially and temporally in precise patterns is Atoh1, a transcription factor regulating inner ear hair cell differentiation. Many signaling pathways have been found to regulate *Atoh1* transcription, but until now post-translational regulation of Atoh1 stability had not been studied.

We discovered that Atoh1 was degraded through the ubiquitin-proteasome pathway, as it was stabilized by pharmacological inhibition of proteasome activity. The evolutionarily conserved C-terminus of Atoh1 played an important role in the degradation of Atoh1 acting as a signal for protein degradation (a degron).

We further identified Huwe1, a HECT domain E3 ubiquitin ligase, as a binding partner of Atoh1 by immunoprecipitation/mass spectrometry, and we proved the identity of the E3 ligase by reciprocal immunoprecipitation. Gain-of-function and loss-of-function assays both showed that Huwe1 was responsible for Atoh1 stability. In-vivo ubiquitylation also showed that Huwe1 was involved, and mutation at cysteine 434 of Huwe1 caused decreased ubiquitin transfer. Similarly, impaired Huwe1 binding as well as decreased ubiquitylation were also observed for degron-deleted Atoh1. Proteasome inhibition and *Huwe1* knockdown stabilized Atoh1, and, importantly, increased hair cell genesis in the cochlea.

Thesis conclusions

Significance

The overall goal of this research was to enhance hair cell differentiation by manipulation of the ubiquitin-proteasome pathway regulating Atoh1 and, ultimately, to apply this knowledge to inner ear regeneration. We demonstrate that specific inhibition of the ubiquitin-proteasome pathway stabilized the level of Atoh1 and enhanced hair cell formation in the cochlea. The work has led to a better understanding of the post-translational regulation of Atoh1 and provides a biochemical basis that can ultimately lead to clinical interventions for replacement of hair cells in a damaged cochlea.

Innovation

In this research, we tested hypotheses that Atoh1 was stabilized through regulation of the ubiquitin-proteasome pathway and that post-translational stabilization of Atoh1 could enhance hair cell formation.

Atoh1 stabilization through regulation of the ubiquitin-proteasome pathway

E3-ubiquitin ligases transfer ubiquitin to specific proteins, conferring substrate specificity to the proteasome. Accumulating evidence reveals that the ubiquitin-proteasome pathway plays an important role in the division, differentiation, and survival of stem cell and progenitor populations via proteolytic degradation of key regulatory proteins of signaling pathways (Naujokat and Šarić, 2007).

Most attempts to achieve hair cell regeneration have addressed transcriptional regulation of *Atoh1* through signaling pathways. Post-translational regulation of Atoh1 has not been studied. We show that Atoh1 is regulated by the ubiquitin-proteasome pathway in the inner ear.

We characterize the specific ubiquitin ligase targeting Atoh1 by biochemical approaches and assess its potential function in regulation of Atoh1. We also identify a specific Atoh1 sequence recognized by the E3 ligase.

Inner ear regeneration through ubiquitin-proteasomal regulation of Atoh1

We develop a new strategy to regenerate inner ear hair cells through ubiquitin-proteasomal regulation of Atoh1. Targeting an Atoh1-specific ubiquitin ligase allows post-translational stabilization of Atoh1; we show that this is a novel route to hair cell differentiation.

Future directions

Atoh1 is necessary for hair cell differentiation during development and for differentiation of stem cells. My research has uncovered a ubiquitin-proteasome signaling pathway regulating Atoh1 protein post-translationally. Our identification of Huwe1-ubiquitylation of Atoh1 is useful for the study of the mechanism of Atoh1 regulation in the inner ear. I am currently investigating the role of Huwe1 during hair cell development as well as hair cell regeneration in order to gain deeper knowledge and insight into its impact. Ultimately, we will apply the knowledge from this research to a new treatment modality of hearing loss.

Huwe1 during inner ear development

Since Huwe1, in addition to Atoh1, regulates other transcription factors, such as N-Myc and p53, it may prove interesting to see if Huwe1 acts on other factors in inner ear development. The use of genetic models that specifically shut down *Huwe1* expression in the inner ear would allow us to test the role of Huwe1 during development.

In vivo work

Having found that *Huwe1* knockdown in the *ex vivo* organ of Corti explants increases hair cell genesis, we are now investigating the effect of *Huwe1* knockdown in *in vivo* models in the adult cochlea to see if similar results can be achieved. An RNA interference-based gene therapy targeting the specific E3-ligase that regulates Atoh1 could potentially create new hair cells. In addition, we will determine whether new small molecule inhibitors of Huwe1 can be obtained by compound screening. Thus, treatments targeting *Huwe* are promising new approaches to hair cell regeneration

References

Abbott DW, Yang Y, Hutti JE, Madhavarapu S, Kelliher MA, Cantley LC (2007) Coordinated regulation of Toll-like receptor and NOD2 signaling by K63-linked polyubiquitin chains. Molecular and Cellular Biology 27:6012-6025.

Adhikary S, Marinoni F, Hock A, Hulleman E, Popov N, Beier R, Bernard S, Quarto M, Capra M, Goettig S, Kogel U, Scheffner M, Helin K, Eilers M (2005) The ubiquitin ligase HectH9 regulates transcriptional activation by Myc and is essential for tumor cell proliferation. Cell 123:409-421.

Adler HJ, Raphael Y (1996) New hair cells arise from supporting cell conversion in the acoustically damaged chick inner ear. Neuroscience letters 205:17-20.

Barker N, van Es J, Kuipers J, Kujala P, van den Born M, Cozijnsen M, Haegebarth A, Korving J, Begthel H, Peters P (2007) Identification of stem cells in small intestine and colon by marker gene Lgr5. Nature 449:1003-1007.

Ben-Arie N, Bellen HJ, Armstrong DL, McCall AE, Gordadze PR, Guo Q, Matzuk MM, Zoghbi HY (1997) Math1 is essential for genesis of cerebellar granule neurons. Nature 390:169-172.

Ben-Arie N, Hassan BA, Bermingham NA, Malicki DM, Armstrong D, Matzuk M, Bellen HJ, Zoghbi HY (2000) Functional conservation of atonal and Math1 in the CNS and PNS. Development (Cambridge, England) 127:1039-1048.

Bermingham NA, Hassan BA, Price SD, Vollrath MA, Ben-Arie N, Eatock RA, Bellen HJ, Lysakowski A, Zoghbi HY (1999) Math1: an essential gene for the generation of inner ear hair cells. Science (New York, NY) 284:1837-1841.

Bertrand N, Castro D, Guillemot F (2002) Proneural genes and the specification of neural cell types. Nature Reviews Neuroscience 3:517-530.

Bossuyt W, Kazanjian A, De Geest N, Van Kelst S, De Hertogh G, Geboes K, Boivin GP, Luciani J, Fuks F, Chuah M, VandenDriessche T, Marynen P, Cools J, Shroyer NF, Hassan BA (2009) Atonal homolog 1 is a tumor suppressor gene. PLoS biology 7:e39.

Bramhall NF, Shi F, Arnold K, Hochedlinger K, Edge ASB (2014) Lgr5-positive supporting cells generate new hair cells in the postnatal cochlea. Stem cell reports 2:311-322.

Brooker R, Hozumi K, Lewis J (2006) Notch ligands with contrasting functions: Jagged1 and Delta1 in the mouse inner ear. Development (Cambridge, England) 133:1277-1286.

Cafaro J, Lee GS, Stone JS (2007) Atoh1 expression defines activated progenitors and differentiating hair cells during avian hair cell regeneration. Developmental dynamics : an official publication of the American Association of Anatomists 236:156-170.

Cai T, Seymour ML, Zhang H, Pereira FA, Groves AK (2013) Conditional deletion of Atoh1 reveals distinct critical periods for survival and function of hair cells in the organ of Corti. The Journal of neuroscience : the official journal of the Society for Neuroscience 33:10110-10122.

Chen D, Kon N, Li M, Zhang W, Qin J, Gu W (2005) ARF-BP1/Mule is a critical mediator of the ARF tumor suppressor. Cell 121:1071-1083.

Chen P, Johnson JE, Zoghbi HY, Segil N (2002) The role of Math1 in inner ear development: Uncoupling the establishment of the sensory primordium from hair cell fate determination. Development (Cambridge, England) 129:2495-2505.

Clevers H (2006) Wnt/beta-catenin signaling in development and disease. Cell 127:469-480.

Corwin JT, Cotanche DA (1988) Regeneration of sensory hair cells after acoustic trauma. Science (New York, NY) 240:1772-1774.

D'Arca D, Zhao X, Xu W, Ramirez-Martinez NC, Iavarone A, Lasorella A (2010) Huwe1 ubiquitin ligase is essential to synchronize neuronal and glial differentiation in the developing cerebellum. Proceedings of the National Academy of Sciences of the United States of America 107:5875-5880.

Davis AC (1983) Hearing disorders in the population: first phase findings of the MRC National Study of Hearing. Hearing science and hearing disorders 35.

de Groot REA, Ganji RS, Bernatik O, Lloyd-Lewis B, Seipel K, Šedová K, Zdráhal Z, Dhople VM, Dale TC, Korswagen HC, Bryja V (2014) Huwe1-mediated ubiquitylation of dishevelled defines a negative feedback loop in the Wnt signaling pathway. Science signaling 7:ra26.

Deshaies RJ, Joazeiro CAP (2009) RING domain E3 ubiquitin ligases. Annual review of biochemistry 78:399-434.

Eng JK, McCormack AL, Yates JR (1994) An approach to correlate tandem mass spectral data of peptides with amino acid sequences in a protein database. Journal of the American Society for Mass Spectrometry 5:976-989.

Flora A, Garcia J, Thaller C, Zoghbi H (2007) The E-protein Tcf4 interacts with Math1 to regulate differentiation of a specific subset of neuronal progenitors. Proceedings of the National Academy of Sciences 104:15382.

Flora A, Klisch TJ, Schuster G, Zoghbi HY (2009) Deletion of Atoh1 disrupts Sonic Hedgehog signaling in the developing cerebellum and prevents medulloblastoma. Science (New York, NY) 326:1424-1427.

Forge A, Li L, Corwin JT, Nevill G (1993) Ultrastructural evidence for hair cell regeneration in the mammalian inner ear. Science (New York, NY) 259:1616-1619.

Fritzsch B (2003) Development of inner ear afferent connections: forming primary neurons and connecting them to the developing sensory epithelia. Brain research bulletin 60:423-433.

Gao D, Inuzuka H, Tan M-KM, Fukushima H, Locasale JW, Liu P, Wan L, Zhai B, Chin YR, Shaik S, Lyssiotis CA, Gygi SP, Toker A, Cantley LC, Asara JM, Harper JW, Wei W (2011a) mTOR drives its own activation via SCF(βTrCP)-dependent degradation of the mTOR inhibitor DEPTOR. Molecular cell 44:290-303.

Gao SS, Xia A, Yuan T, Raphael PD, Shelton RL, Applegate BE, Oghalai JS (2011b) Quantitative imaging of cochlear soft tissues in wild-type and hearing-impaired transgenic mice by spectral domain optical coherence tomography. Optics express 19:15415-15428.

Gregorieff A, Clevers H (2005) Wnt signaling in the intestinal epithelium: from endoderm to cancer. Genes & development 19:877-890.

Gubbels SP, Woessner DW, Mitchell JC, Ricci AJ, Brigande JV (2008) Functional auditory hair cells produced in the mammalian cochlea by in utero gene transfer. Nature 455:537-541.

Herold S, Hock A, Herkert B, Berns K, Mullenders J, Beijersbergen R, Bernards R, Eilers M (2008) Miz1 and HectH9 regulate the stability of the checkpoint protein, TopBP1. The EMBO Journal 27:2851-2861.

Hirabayashi Y, Itoh Y, Tabata H, Nakajima K, Akiyama T, Masuyama N, Gotoh Y (2004) The Wnt/beta-catenin pathway directs neuronal differentiation of cortical neural precursor cells. Development (Cambridge, England) 131:2791-2801.

Hu Z, Ulfendahl M (2006) Cell replacement therapy in the inner ear. Stem cells and development 15:449-459.

Hu Z, Andäng M, Ni D, Ulfendahl M (2005) Neural cograft stimulates the survival and differentiation of embryonic stem cells in the adult mammalian auditory system. Brain Research 1051:137-144.

Huang F, Zeng X, Kim W, Balasubramani M, Fortian A, Gygi SP, Yates NA, Sorkin A (2013) Lysine 63-linked polyubiquitination is required for EGF receptor degradation. Proceedings of the National Academy of Sciences of the United States of America 110:15722-15727.

Huibregtse JM, Scheffner M, Beaudenon S, Howley PM (1995) A family of proteins structurally and functionally related to the E6-AP ubiquitin-protein ligase. Proceedings of the National Academy of Sciences of the United States of America 92:5249.

Husseman J, Raphael Y (2009) Gene therapy in the inner ear using adenovirus vectors. Advances in oto-rhino-laryngology 66:37-51.

Ikeda F, Dikic I (2008) Atypical ubiquitin chains: new molecular signals. "Protein Modifications: Beyond the Usual Suspects" review series. EMBO Reports 9:536-542.

Incesulu A, Nadol JB (1998) Correlation of acoustic threshold measures and spiral ganglion cell survival in severe to profound sensorineural hearing loss: implications for cochlear implantation. The Annals of otology, rhinology, and laryngology 107:906-911.

Inoue S et al. (2013) Mule/Huwe1/Arf-BP1 suppresses Ras-driven tumorigenesis by preventing c-Myc/Miz1-mediated down-regulation of p21 and p15. Genes & development 27:1101-1114.

Inuzuka H, Shaik S, Onoyama I, Gao D, Tseng A, Maser RS, Zhai B, Wan L, Gutierrez A, Lau AW, Xiao Y, Christie AL, Aster J, Settleman J, Gygi SP, Kung AL, Look T, Nakayama KI, Depinho RA, Wei W (2012) SCFFBW7 regulates cellular apoptosis by targeting MCL1 for ubiquitylation and destruction. Nature 470:104-109.

Ivan M, Kondo K, Yang H, Kim W, Valiando J, Ohh M, Salic A, Asara JM, Lane WS, Kaelin WG (2001) HIFalpha targeted for VHL-mediated destruction by proline hydroxylation: implications for O2 sensing. Science (New York, NY) 292:464-468.

Izumikawa M, Minoda R, Kawamoto K, Abrashkin KA, Swiderski DL, Dolan DF, Brough DE, Raphael Y (2005) Auditory hair cell replacement and hearing improvement by Atoh1 gene therapy in deaf mammals. Nature Medicine 11:271-276.

Jaakkola P, Mole DR, Tian YM, Wilson MI, Gielbert J, Gaskell SJ, von Kriegsheim A, Hebestreit HF, Mukherji M, Schofield CJ, Maxwell PH, Pugh CW, Ratcliffe PJ (2001) Targeting of HIF-alpha to the von Hippel-Lindau ubiquitylation complex by O2-regulated prolyl hydroxylation. Science (New York, NY) 292:468-472.

Jarriault S, Brou C, Logeat F, Schroeter EH, Kopan R, Israel A (1995) Signalling downstream of activated mammalian Notch. Nature 377:355-358.

Jeon S-J, Oshima K, Heller S, Edge ASB (2007) Bone marrow mesenchymal stem cells are progenitors in vitro for inner ear hair cells. Molecular and cellular neurosciences 34:59-68.

Jeon S-J, Fujioka M, Kim S-C, Edge ASB (2011) Notch signaling alters sensory or neuronal cell fate specification of inner ear stem cells. The Journal of neuroscience : the official journal of the Society for Neuroscience 31:8351-8358.

Kawamoto K, Izumikawa M, Beyer LA, Atkin GM, Raphael Y (2009) Spontaneous hair cell regeneration in the mouse utricle following gentamicin ototoxicity. Hearing research 247:17-26.

Kelley MW (2006) Regulation of cell fate in the sensory epithelia of the inner ear. Nature Reviews Neuroscience 7:837-849.

Klisch TJ, Xi Y, Flora A, Wang L, Li W, Zoghbi HY (2011) In vivo Atoh1 targetome reveals how a proneural transcription factor regulates cerebellar development. Proceedings of the National Academy of Sciences of the United States of America.

Knippschild U, Krüger M, Richter J, Xu P, García-Reyes B, Peifer C, Halekotte J, Bakulev V, Bischof J (2014) The CK1 Family: Contribution to Cellular Stress Response and Its Role in Carcinogenesis. Frontiers in oncology 4:96.

Kondo T, Matsuoka AJ, Shimomura A, Koehler KR, Chan RJ, Miller JM, Srour EF, Hashino E (2011) Wnt Signaling Promotes Neuronal Differentiation From Mesenchymal Stem Cells Through Activation of Tlx3. Stem cells (Dayton, Ohio).

Kurokawa M, Kim J, Geradts J, Matsuura K, Liu L, Ran X, Xia W, Ribar TJ, Henao R, Dewhirst MW, Kim W-J, Lucas JE, Wang S, Spector NL, Kornbluth S (2013) A network of substrates of the E3 ubiquitin ligases MDM2 and HUWE1 control apoptosis independently of p53. Science signaling 6:ra32.

Lanford PJ, Lan Y, Jiang R, Lindsell C, Weinmaster G, Gridley T, Kelley MW (1999) Notch signalling pathway mediates hair cell development in mammalian cochlea. Nature Genetics 21:289-292.

Latres E, Chiaur DS, Pagano M (1999) The human F box protein beta-Trcp associates with the Cul1/Skp1 complex and regulates the stability of beta-catenin. Oncogene 18:849-854.

Ledent V, Paquet O, Vervoort M (2002) Phylogenetic analysis of the human basic helix-loop-helix proteins. Genome biology 3:RESEARCH0030.

Lee JM, Lee JS, Kim H, Kim K, Park H, Kim J-Y, Lee SH, Kim IS, Kim J, Lee M, Chung CH, Seo S-B, Yoon J-B, Ko E, Noh D-Y, Kim KI, Kim KK, Baek SH (2012) EZH2 generates a methyl degron that is recognized by the DCAF1/DDB1/CUL4 E3 ubiquitin ligase complex. Molecular cell 48:572-586.

Lin V, Golub JS, Nguyen TB, Hume CR, Oesterle EC, Stone JS (2011) Inhibition of notch activity promotes nonmitotic regeneration of hair cells in the adult mouse utricles. The Journal of neuroscience : the official journal of the Society for Neuroscience 31:15329-15339.

Lo LC, Johnson JE, Wuenschell CW, Saito T, Anderson DJ (1991) Mammalian achaete-scute homolog 1 is transiently expressed by spatially restricted subsets of early neuroepithelial and neural crest cells. Genes & development 5:1524-1537.

Ma EY, Raible DW (2009) Signaling pathways regulating zebrafish lateral line development. Current biology : CB 19:R381-386.

Maksimovic S, Nakatani M, Baba Y, Nelson AM, Marshall KL, Wellnitz SA, Firozi P, Woo S-H, Ranade S, Patapoutian A, Lumpkin EA (2014) Epidermal Merkel cells are mechanosensory cells that tune mammalian touch receptors. Nature 509:617-621.

Markkanen E, van Loon B, Ferrari E, Parsons JL, Dianov GL, Hübscher U (2012) Regulation of oxidative DNA damage repair by DNA polymerase λ and MutYH by cross-talk of phosphorylation and ubiquitination. Proceedings of the National Academy of Sciences of the United States of America 109:437-442.

Meierhofer D, Wang X, Huang L, Kaiser P (2008) Quantitative analysis of global ubiquitination in HeLa cells by mass spectrometry. Journal of proteome research 7:4566-4576.

Miesegaes GR, Klisch TJ, Thaller C, Ahmad KA, Atkinson RC, Zoghbi HY (2009) Identification and subclassification of new Atoh1 derived cell populations during mouse spinal cord development. Developmental Biology 327:339-351.

Mizutari K, Fujioka M, Hosoya M, Bramhall N, Okano HJ, Okano H, Edge ASB (2013) Notch inhibition induces cochlear hair cell regeneration and recovery of hearing after acoustic trauma. Neuron 77:58-69.

Morrison KM, Miesegaes GR, Lumpkin EA, Maricich SM (2009) Mammalian Merkel cells are descended from the epidermal lineage. Developmental Biology 336:76-83.

Murre C, McCaw PS, Vaessin H, Caudy M, Jan LY, Jan YN, Cabrera CV, Buskin JN, Hauschka SD, Lassar AB (1989) Interactions between heterologous helix-loop-helix proteins generate complexes that bind specifically to a common DNA sequence. Cell 58:537-544.

Naujokat C, Šarić T (2007) Concise review: role and function of the ubiquitin-proteasome system in mammalian stem and progenitor cells. Stem cells (Dayton, Ohio) 25:2408-2418.

Noy T, Suad O, Taglicht D, Ciechanover A (2012) HUWE1 ubiquitinates MyoD and targets it for proteasomal degradation. Biochemical and Biophysical Research Communications 418:408-413.

Ohyama T, Mohamed OA, Taketo MM, Dufort D, Groves AK (2006) Wnt signals mediate a fate decision between otic placode and epidermis. Development (Cambridge, England) 133:865-875.

Pan N, Jahan I, Kersigo J, Duncan JS, Kopecky B, Fritzsch B (2012) A novel Atoh1 "self-terminating" mouse model reveals the necessity of proper Atoh1 level and duration for hair cell differentiation and viability. PloS one 7:e30358.

Pandya RK, Partridge JR, Love KR, Schwartz TU, Ploegh HL (2010) A structural element within the HUWE1 HECT domain modulates self-ubiquitination and substrate ubiquitination activities. The Journal of biological chemistry 285:5664-5673.

Parker M, Brugeaud A, Edge ASB (2010) Primary culture and plasmid electroporation of the murine organ of Corti. Journal of Visualized Experiments.

Parker MA (2011) Biotechnology in the treatment of sensorineural hearing loss: foundations and future of hair cell regeneration. Journal of speech, language, and hearing research : JSLHR 54:1709-1731.

Parker MA, Cheng Y-f, Kinouchi H, Bieber R, Edge ASB (2014) An independent construct for conditional expression of atonal homolog-1. Human gene therapy methods 25:1-13.

Peng J, Schwartz D, Elias JE, Thoreen CC, Cheng D, Marsischky G, Roelofs J, Finley D, Gygi SP (2003) A proteomics approach to understanding protein ubiquitination. Nature Biotechnology 21:921-926.

Qyang Y, Martin-Puig S, Chiravuri M, Chen S, Xu H, Bu L, Jiang X, Lin L, Granger A, Moretti A, Caron L, Wu X, Clarke J, Taketo MM, Laugwitz K-L, Moon RT, Gruber P, Evans SM, Ding S, Chien KR (2007) The renewal and differentiation of Isl1+ cardiovascular progenitors are controlled by a Wnt/beta-catenin pathway. Cell stem cell 1:165-179.

Riccomagno M, Takada S, Epstein D (2005) Wnt-dependent regulation of inner ear morphogenesis is balanced by the opposing and supporting roles of Shh. Genes & development 19:1612-1623.

Roberson DW, Alosi JA, Cotanche DA (2004) Direct transdifferentiation gives rise to the earliest new hair cells in regenerating avian auditory epithelium. Journal of neuroscience research 78:461-471.

Ross SE, Greenberg ME, Stiles CD (2003) Basic helix-loop-helix factors in cortical development. Neuron 39:13-25.

Rotin D, Kumar S (2009) Physiological functions of the HECT family of ubiquitin ligases. Nature Reviews Molecular Cell Biology 10:398-409.

Scheffner M, Staub O (2007) HECT E3s and human disease. BMC biochemistry 8 Suppl 1:S6.

Schwarz SE, Rosa JL, Scheffner M (1998) Characterization of human hect domain family members and their interaction with UbcH5 and UbcH7. The Journal of biological chemistry 273:12148-12154.

Shi F, Kempfle JS, Edge ASB (2012) Wnt-responsive Lgr5-expressing stem cells are hair cell progenitors in the cochlea. The Journal of neuroscience : the official journal of the Society for Neuroscience 32:9639-9648.

Shi F, Cheng Y-f, Wang XL, Edge ASB (2010) Beta-catenin up-regulates Atoh1 expression in neural progenitor cells by interaction with an Atoh1 3' enhancer. The Journal of biological chemistry 285:392-400.

Shi F, Hu L, Jacques BE, Mulvaney JF, Dabdoub A, Edge ASB (2014) β-Catenin is required for hair-cell differentiation in the cochlea. The Journal of neuroscience : the official journal of the Society for Neuroscience 34:6470-6479.

Skowyra D, Craig KL, Tyers M, Elledge SJ, Harper JW (1997) F-box proteins are receptors that recruit phosphorylated substrates to the SCF ubiquitin-ligase complex. Cell 91:209-219.

Sowa ME, Bennett EJ, Gygi SP, Harper JW (2009) Defining the human deubiquitinating enzyme interaction landscape. Cell 138:389-403.

Spence J, Sadis S, Haas AL, Finley D (1995) A ubiquitin mutant with specific defects in DNA repair and multiubiquitination. Molecular and Cellular Biology 15:1265-1273.

Staecker H, Praetorius M, Baker K, Brough DE (2007) Vestibular hair cell regeneration and restoration of balance function induced by math1 gene transfer. Otology & neurotology 28:223-231.

Stevens CB, Davies AL, Battista S, Lewis JH, Fekete DM (2003) Forced activation of Wnt signaling alters morphogenesis and sensory organ identity in the chicken inner ear. Developmental Biology 261:149-164.

Stone JS, Cotanche DA (1994) Identification of the timing of S phase and the patterns of cell proliferation during hair cell regeneration in the chick cochlea. The Journal of Comparative Neurology 341:50-67.

Tai H-C, Schuman EM (2008) Ubiquitin, the proteasome and protein degradation in neuronal function and dysfunction. Nature Reviews Neuroscience 9:826-838.

Takebayashi S, Yamamoto N, Yabe D, Fukuda H, Kojima K, Ito J, Honjo T (2007) Multiple roles of Notch signaling in cochlear development. Developmental Biology 307:165-178.

Tan M-KM, Lim H-J, Bennett EJ, Shi Y, Harper JW (2013) Parallel SCF adaptor capture proteomics reveals a role for SCFFBXL17 in NRF2 activation via BACH1 repressor turnover. Molecular cell 52:9-24.

Tiveron MC, Pattyn A, Hirsch MR, Brunet JF (2003) Role of Phox2b and Mash1 in the generation of the vestibular efferent nucleus. Developmental Biology 260:46-57.

Tsuchiya K, Nakamura T, Okamoto R, Kanai T, Watanabe M (2007) Reciprocal targeting of Hath1 and beta-catenin by Wnt glycogen synthase kinase 3beta in human colon cancer. Gastroenterology 132:208-220.

Varshavsky A (1991) Naming a targeting signal. Cell 64:13-15.

Wang X, Lu G, Li L, Yi J, Yan K, Wang Y, Zhu B, Kuang J, Lin M, Zhang S, Shao G (2013) HUWE1 interacts with BRCA1 and promotes its degradation in the ubiquitin-proteasome pathway. Biochemical and Biophysical Research Communications.

Warchol ME, Lambert PR, Goldstein BJ, Forge A, Corwin JT (1993) Regenerative proliferation in inner ear sensory epithelia from adult guinea pigs and humans. Science (New York, NY) 259:1619-1622.

WHO In.

Woods C, Montcouquiol M, Kelley MW (2004) Math1 regulates development of the sensory epithelium in the mammalian cochlea. Nature Neuroscience 7:1310.

Wu G, Xu G, Schulman BA, Jeffrey PD, Harper JW, Pavletich NP (2003) Structure of a beta-TrCP1-Skp1-beta-catenin complex: destruction motif binding and lysine specificity of the SCF(beta-TrCP1) ubiquitin ligase. Molecular cell 11:1445-1456.

Yamamoto N, Tanigaki K, Tsuji M, Yabe D, Ito J, Honjo T (2006) Inhibition of Notch/RBP-J signaling induces hair cell formation in neonate mouse cochleas. Journal of Molecular Medicine 84:37-45.

Yang H, Xie X, Deng M, Chen X, Gan L (2010a) Generation and characterization of Atoh1-Cre knock-in mouse line. Genesis (New York, NY : 2000) 48:407-413.

Yang Q, Bermingham N, Finegold M, Zoghbi H (2001) Requirement of Math1 for Secretory Cell Lineage Commitment in the Mouse Intestine. Science (New York, NY) 294:2155.

Yang Y, Do H, Tian X, Zhang C, Liu X, Dada LA, Sznajder JI, Liu J (2010b) E3 ubiquitin ligase Mule ubiquitinates Miz1 and is required for TNFalpha-induced JNK activation. Proceedings of the National Academy of Sciences of the United States of America 107:13444-13449.

Ye X, Nalepa G, Welcker M, Kessler BM, Spooner E, Qin J, Elledge SJ, Clurman BE, Harper JW (2004) Recognition of phosphodegron motifs in human cyclin E by the SCF(Fbw7) ubiquitin ligase. The Journal of biological chemistry 279:50110-50119.

Zhang J, Kan S, Huang B, Hao Z, Mak TW, Zhong Q (2011) Mule determines the apoptotic response to HDAC inhibitors by targeted ubiquitination and destruction of HDAC2. Genes & development 25:2610-2618.

Zhao X, Heng JI-T, Guardavaccaro D, Jiang R, Pagano M, Guillemot F, Iavarone A, Lasorella A (2008) The HECT-domain ubiquitin ligase Huwe1 controls neural differentiation and proliferation by destabilizing the N-Myc oncoprotein. Nature Cell Biology 10:643-653.

Zhao X, D'Arca D, Lim WK, Brahmachary M, Carro MS, Ludwig T, Cardo CC, Guillemot F, Aldape K, Califano A, Iavarone A, Lasorella A (2009) The N-Myc-DLL3 cascade is suppressed by the ubiquitin ligase Huwe1 to inhibit proliferation and promote neurogenesis in the developing brain. Developmental cell 17:210-221.

Zheng JL, Gao W-Q (2000) Overexpression of Math1 induces robust production of extra hair cells in postnatal rat inner ears. Nature Neuroscience 3:580.

Zhong Q, Gao W, Du F, Wang X (2005) Mule/ARF-BP1, a BH3-only E3 ubiquitin ligase, catalyzes the polyubiquitination of Mcl-1 and regulates apoptosis. Cell 121:1085-1095.

Addendum

During the writing of my thesis, a paper came out on Atoh1 stability in the cerebellum (Forget et al., 2014). The authors suggested that Huwe1 acted as an E3 ligase for Atoh1 and hypothesized that sonic hedgehog (SHH) prevented phosphorylation-dependent degradation of Atoh1 by Huwe1.

Since these results have some similarities to the data in this thesis, we have summarized the data here and pointed out several differences.

1. Different systems: A major difference is that cerebellar Atoh1 is part of a positive regulatory loop that drives proliferation of cerebellar neural progenitors, while hair cell precursors exit the cell cycle immediately after Atoh1 is expressed in the cochlea during embryonic development. Atoh1 is downstream of SHH in the cerebellum, whereas Atoh1 in the inner ear is regulated by Wnt signaling and is modulated by Notch. SHH inhibits hair cell differentiation in the embryo. Given the important role of Atoh1 in hair cell differentiation, these data suggest that the regulation of Atoh1 by SHH in the inner ear is distinctly different from the brain.

2. **Proof of the ubiquitylation by Huwe1**:

The paper of Forget et al. uses siRNA silencing and Huwe1 knockout to prove that Huwe1 influences Atoh1 stability. Knockout studies have a limited utility for identification of the mechanism of action for critical genes that affect multiple pathways. The stabilization of Atoh1 in response to knockout of Huwe1 may not be direct, as suggested by these authors. Signaling molecules that play important roles in the generation of neurons and sensory cells, such as N-myc, p53, and disheveled, are Huwe1 targets that could be upstream of *Atoh1* and

would alter its level if upregulated by Huwe1 silencing. Thus, without evidence from a cell-free assay, in which the enzyme activity is demonstrated *in vitro*, it is not possible to rule out an indirect effect through one of these targets.

We are testing Huwe1 ubiquitylation of Atoh1 to make this determination in such a cell-free system. If Huwe1 is an Atoh1 E3 ubiquitin ligase, polyubiquitin chains will be transferred to Atoh1 upon adding recombinant Huwe1 protein, but not in its absence, in a reconstituted cell-free system containing recombinant GST-Atoh1 with E1, E2 (UbcH5a), ubiquitin, and a cocktail for regenerating ATP.

3. **Differences in the postulated residues that target Atoh1 for degradation**: Forget et al. suggested that two phosphorylated serine residues, S328 and S339, were involved in Atoh1 degradation and interaction with Huwe1. The half-life of Atoh1 for mutants S328A, S339A and the double mutant was extended (100, 130 and 240 minutes respectively) compared to wild-type (38 minutes). We found that the mutation at serine 334 (S334A) caused the most-extended half-life (81.79 as compared to 48.86 minutes for S328). Serines 328 and 339 are located in the C-terminus of Atoh1 within the degron motif that we identified. Serine 339 was not one of the candidate residues tested because it is not conserved in all species. S334 is conserved (see Figure 2-5).

4. **Kinase identification**: We have identified a candidate kinase that may catalyze the phosphorylation of the serine residue (serine 334) critical for Atoh1 stability as casein kinase 1 (see Figure 2-5 and chapter 3 discussion).

5. **Huwe1 ubiquitylates Atoh1 through a K48 linkage tagging it for proteasomal degradation in vivo (see Figure 3-3)**: Forget et al. suggested that Huwe1 was involved in the stability of Atoh1, but their study failed to provide direct evidence that Huwe1 promoted proteasomal degradation of Atoh1 through a K48 polyubiquitin chain (see Figure 2-3 and 3-3). As discussed in chapter 3, Huwe1 might be involved in other biological functions such as subcellular trafficking by forming K11 or K63-linked polyubiquitin chain to substrates. Thus, SHH may regulate Atoh1 biological activities through phosphorylated sites (S328 and S339) may be required for ubiquitylation of Atoh1 by other linkages such as K63 or K11.

Reference

Forget A, Bihannic L, Cigna SM, Lefevre C, Remke M, Barnat M, Dodier S, Shirvani H, Mercier A, Mensah A, Garcia M, Humbert S, Taylor MD, Lasorella A, Ayrault O (2014) Shh Signaling Protects Atoh1 from Degradation Mediated by the E3 Ubiquitin Ligase Huwe1 in Neural Precursors. Developmental cell 29:649-661.